Graphical abstract

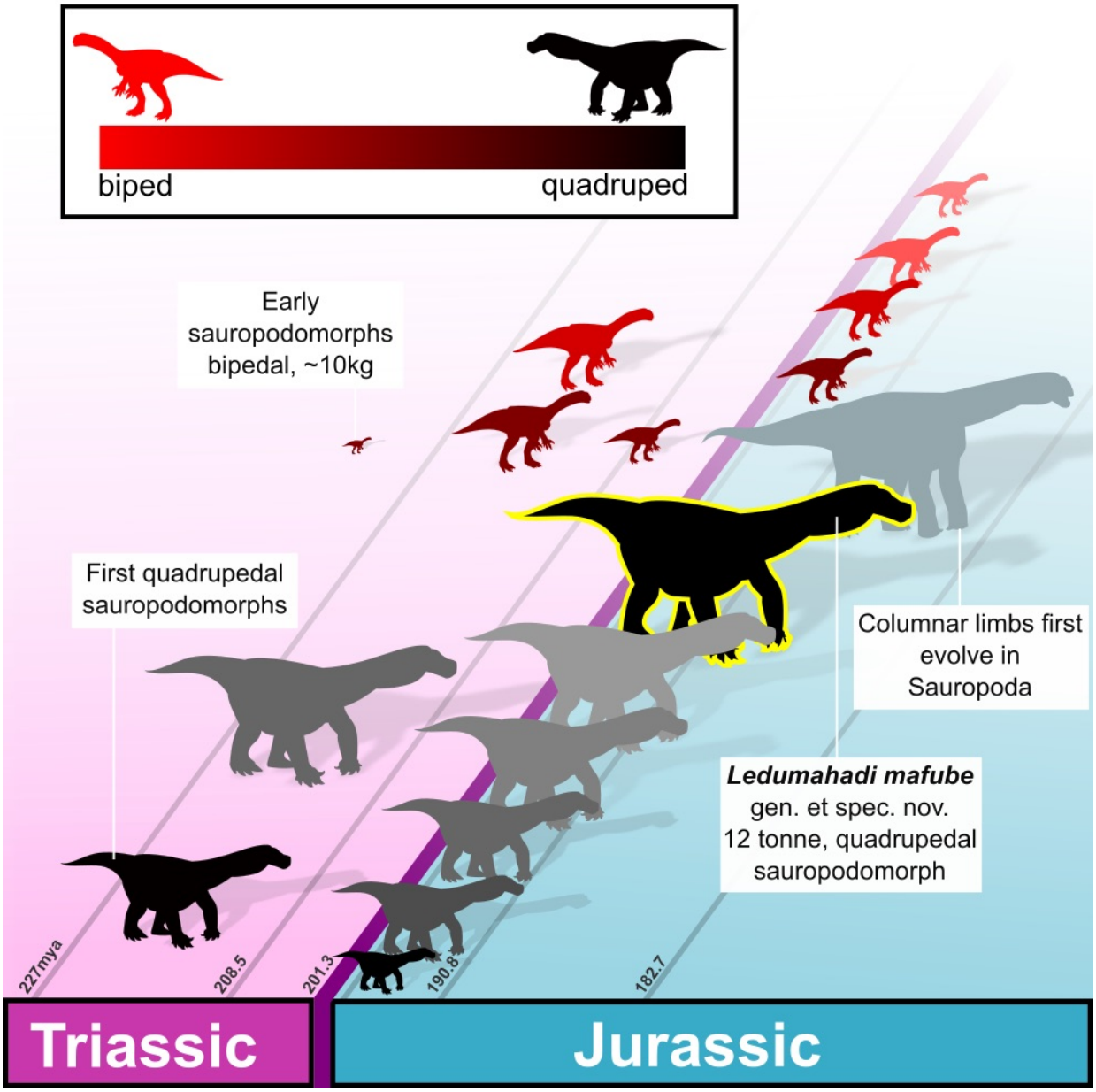

McPhee et al, 2018: A giant dinosaur from the earliest Jurassic of South Africa and the transition to quadrupedality in early sauropodomorphs

eTOC Blurb

McPhee et al. present a new, gigantic sauropodomorph dinosaur and a quantitative method for inferring postures in extinct tetrapods using proportional limb robusticity. Quadrupedal postures with flexed limbs evolved potentially several times in sauropodomorph dinosaurs before the evolution of derived, columnar-limbed postures of Sauropoda.

Highlights

- A new species of Early Jurassic South African sauropodomorph weighed 12 tonnes.
- Proportional limb robusticity is useful for inferring posture in extinct tetrapods.
- Many early branching sauropodomorphs were quadrupeds with flexed limbs.
- Quadrupedality evolves at low body mass but facilitates larger body masses.

A giant dinosaur from the earliest Jurassic of South Africa and the transition to quadrupedality in early sauropodomorphs

Blair W. McPhee[1,2], Roger B. J. Benson[2,3], Jennifer Botha-Brink[4,5], Emese M. Bordy[6], Jonah N. Choiniere[2,*]

[1]Departamento de Biologia, FFCLRP, Universidade de São Paulo, Ribeirão Preto, Brasil.

[2]Evolutionary Studies Institute, University of the Witwatersrand, Johannesburg, South Africa

[3]Department of Earth Sciences, University of Oxford, Oxford, UK

[4]National Museum, Bloemfontein, South Africa

[5]Department of Zoology and Entomology, University of the Free State, Bloemfontein, Bloemfontein, South Africa 9300

[6]Department of Geological Sciences, University of Cape Town, Cape Town, South Africa

*Lead contact: Jonah.Choiniere@wits.ac.za

SUMMARY

Sauropod dinosaurs were dominant, bulk-browsing herbivores for 130 million years of the Mesozoic, attaining gigantic body masses in excess of 60 tonnes [1, 2]. A columnar-limbed, quadrupedal posture enabled these giant body sizes [3], but the nature of the transition from bipedal sauropodomorph ancestors to derived quadrupeds remains contentious [4-6]. We describe a gigantic, new sauropodomorph from the earliest Jurassic of South Africa weighing 12 tonnes, and representing a phylogenetically independent origin of sauropod-like body size in a non-sauropod. Osteohistological evidence shows that this specimen was an adult of maximum size and approximately 14 years old at death. *Ledumahadi mafube* gen. et sp. nov. shows that gigantic body sizes were possible in early sauropodomorphs, which were habitual quadrupeds but lacked the derived, columnar limb postures of sauropods. We use data from this new taxon and a discriminant analysis of tetrapod limb measurements to study postural evolution in sauropodomorphs. Our results show that quadrupedality appeared by the mid-Late Triassic (Norian), well outside of Sauropoda. Secondary reversion to bipedality occurred in some lineages phylogenetically close to Sauropoda, indicating early experimentation in locomotory styles. Morphofunctional observations support the hypothesis that partially flexed (rather than columnar) limbs characterized *Ledumahadi* and other early branching quadrupedal sauropodomorphs. Patterns of locomotory and body size evolution show that quadrupedality allowed Triassic sauropodomorphs to achieve body sizes of at least 3.8 tonnes. *Ledumahadi*'s Early Jurassic age shows that maximum body mass in sauropodomorph dinosaurs was either unaffected or rapidly rebounded after the end-Triassic extinction event.

Keywords: body size, posture, gigantism, columnar limbs

RESULTS

Systematic palaeontology

Saurischia Seeley 1888,

Sauropodomorpha von Huene 1932,

Sauropodiformes Sereno 2007,

Ledumahadi mafube gen. et sp. nov.

Etymology: Southern Sotho. “Ledumahadi”, a giant thunderclap – in recognition of the tremendous size of this taxon; and “mafube”, dawn – in the sense of the stratigraphically early position of this taxon.

Holotype: BP/1/7120: A disarticulated assemblage of associated postcranial material comprising: a partial cervical neural arch; several dorsal vertebrae; partial, conjoined primordial sacral vertebrae; anterior and middle caudal vertebrae; an anterior chevron; a right ulna; a first metacarpal; a left metacarpal, probably III or IV; distal third of the right femur; and a pedal ungual (Figures 1, 4).

Locality and Horizon: Beginsel farm, 25 km SE from the town of Clarens, Free State Province, on the border of South Africa and Lesotho (Figures 1, S1). The *in situ* material was found within mudrocks diagnostic of the upper Elliot Formation, one of the lowermost Jurassic continental successions (Hettangian–Sinemurian, ~200–195 mya; Figures 1, S1).

Diagnosis: *Ledumahadi mafube* possesses several autapomorphies not observed in any other sauropodomorph: (1) medial edge of the proximal surface of the first metacarpal sharply tapering and curved, giving it a sublacriform outline and differing from the typical “keyhole” shape of the proximal first metacarpals of e.g., *Aardonyx, Ingentia*, *Antetonitrus* (Figure 1G); (2) anterior articular facet of the anterior caudal vertebra deeply concave, being set back from

the anterolateral margin of the centrum 4.5 cm at its deepest; and (3) preserved forelimb elements extremely robust, with the minimum shaft circumference of the ulna 0.57 times the total length of the bone (cf. 0.46 in *Antetonitrus*).

Anatomy, Osteohistology, and Systematics

Ledumahadi is known from an incomplete postcranial skeleton that preserves several autapomorphies and generally lacks synapomorphies of Sauropoda, indicating a basal (non-sauropodan) phylogenetic position. The postzygapophysis of the single partial cervical neural arch is not elevated relative to the coronal plane, unlike in *Pulanesaura* and more derived sauropods (Figure 1A) [7]. The neural spine of the anteriormost dorsal vertebra is anteroposteriorly short and expands transversely towards its dorsal apex (Figure 1B). The more posterior dorsal neural spines are proportionately tall for non-sauropodan Sauropodomorpha, with the dorsoventral height approximately twice that of the anteroposterior length of their bases (Figure 1C). They are therefore proportionally taller than those of the large-bodied non-sauropodan sauropodomorph *Antetonitrus*, which are 1.5 times as tall as long [8]. The dorsal neural arches (including spine) are roughly twice the dorsoventral height of their associated centra. The dorsoventral height of the anterior caudal vertebral centrum is 1.7 times its anteroposterior length (Figure 1E). Its anterior face is deeply concave and its posterior face is shallowly convex.

The proximal articular surface of the ulna bears a large olecranon process and a shallow radial fossa, similar to other non-sauropodan sauropodiforms (e.g., *Aardonyx*, *Antetonitrus*, *Lessemsaurus*) (Figure 1F)[8-11]. In contrast, sauropods display a highly reduced olecranon process and much deeper radial fossa (e.g., *Vulcanodon*, *Camarasaurus*)[10]. The anterior tip of the anterior process is deflected medially, similar to the condition seen in *Antetonitrus* [8]. The ulnar shaft is markedly robust (Figures 1, 4). The first metacarpal is extremely stout, with the

mediolateral breadth of the proximal articular surface ~1.1 times the overall length (Figure 1G). This ratio is similar to that of metacarpal I in *Aardonyx* and *Antetonitrus*. However, the proximal outline of metacarpal I is considerably different from those taxa, bearing a sublacriform rather than keyhole shape, and a proportionally longer shaft. The other preserved metacarpal is similarly stout (Figure 1H). Only the distal third of the femur is preserved (Figure 1K). In cross section the shaft is circular, differing from the elliptical (but possibly distorted) cross section of the femur of *Antetonitrus*. The distal condyles are anteroposteriorly expansive and strongly concave ventrally, differing from the anteroposteriorly shortened and flatter distal condyles of sauropod femora (e.g., *Tazoudasaurus* [12]). The single large pedal ungual is likely from the first or second digit (Figure 1I). It has a subcircular proximal outline, similar to the condition of the first and second digits in other late-branching non-sauropodan sauropodomorph taxa such as *Blikanasaurus*.

Osteohistological evidence shows that the holotype of *Ledumahadi* had reached maximum size and was an adult of approximately 14 years of age at its time of death (Figure S2, STAR Methods). *Ledumahadi* exhibited high growth rates during early ontogeny, annual temporary decreases in growth from mid-ontogeny, and a gradual transition to parallel-fibered bone and closely-spaced growth marks near the periphery representing an External Fundamental System (Figure S2, STAR Methods). The closely related sauropodiforms *Lessemsaurus* [13] and *Antetonitrus* [14] also exhibit rapid, but cyclical, growth throughout ontogeny. Given that *Ledumahadi* presents growth marks from at least mid-ontogeny (early growth destroyed by secondary remodeling), it is likely that it grew similarly to these other sauropodiforms. It therefore did not exhibit the sustained growth typical of Sauropoda [13], in spite of its sauropod-like adult body size.

Phylogenetic analysis recovers *Ledumahadi* as sister taxon of another large-bodied upper Elliot Formation taxon, *Antetonitrus ingenipes* (Figures 2, S4, STAR Methods). This is

consistent with the general similarities observed between the two taxa. Nevertheless, the presence of several autapomorphies shows that *Ledumahadi* is distinct from *Antetonitrus* (see *Diagnosis*). Together with the South American taxon *Lessemsaurus* (known from very large, but likely skeletally immature material [11]), these three genera form a monophyletic Lessemsauridae (a fourth member, *Ingentia*, was too recently described [15] to be included in our analysis). Lessemsauridae is within a pectinate grade of non-sauropodan sauropodiforms *sensu* [8], basal to *Leonerasaurus*, *Gongxianosaurus*, *Pulanesaura* and the columnar-limbed quadrupeds known as Sauropoda *sensu* [16; Figures 2, S4].

Body mass estimation and postural determination

The minimum circumferences of limb bone shafts provide information about weight-bearing capacity in tetrapods [17]. Using this relationship for quadrupedal tetrapods [17], the preserved limb elements of BP/1/7120 provide a mass estimate of 12 tonnes for *Ledumahadi mafube* (Figures 2, S3, STAR Methods). Furthermore, skeletal dimensions of *Ledumahadi mafube* are similar to those of geologically younger sauropods including *Jainosaurus* and *Tornieria*. This confidently indicates sauropod-like body size in *L. mafube*, unlike the smaller-bodied sauropodomorphs that have hitherto been known from the earliest Jurassic. *Ledumahadi mafube* is thus the largest animal currently known to have lived on Earth at its time. It is more than three times the size of the largest confidently estimated Late Triassic sauropodomorph (*Camelotia*, 3.8 tonnes; but see [15] for a 7-tonne estimate for *Lessemsaurus*), and considerably larger than the Early Jurassic sauropodomorphs *Antetonitrus* (5.6 tonnes: osteologically immature), and *Vulcanodon* (a sauropod; 10.3 tonnes; ?Sinemurian–Pliensbachian). *Ledumahadi* also extends the total known size range for Early Jurassic Sauropodomorpha, which now spans almost two orders of magnitude, down to a minimum of 0.26 tonnes in *Anchisaurus* (STAR Methods).

To quantify quadrupedality, we used a dataset of humeral and femoral circumferences of 81 dinosaur specimens and hundreds of mammals plus several large-bodied reptiles that are confidently known to have been bipedal or quadrupedal. We used a classification of the predominant mode of locomotion during travel, rather than during slow-speed foraging. For example, kangaroos were classified as bipeds, although they can forage as quadrupeds, and non-human apes were classified as terrestrial quadrupeds (they also use four limbs for arboreal locomotion). Linear discriminant analysis of these data demonstrates that the relationship between the forelimb and hindlimb shaft circumferences can be used to make robust inferences of quadrupedality: a linear discriminant function calibrated using dinosaurs predicts the stances of mammals with a high degree of accuracy, indicating that the method can reliably predict novel datapoints (Figure 3; 90% accuracy, Tables S2, S3). By contrast, lengths of forelimb bones, which have previously been used as evidence of sauropodomorph quadrupedality [9], are unreliable (STAR Methods).

We confidently classify *Ledumahadi* and numerous other sauropodiforms as quadrupeds based on their proportionally robust forelimbs (Figures 1–3, S3, STAR Methods). Phylogenetic optimisation indicates that the transition to quadrupedality occurred during the origins of the clade uniting *Jingshanosaurus* and *Xingxiulong* with more derived sauropodomorphs, and had evolved at least by the mid-Norian, signalled by the occurrence of *Riojasaurus*. Quadrupedal sauropodomorphs have greater maximum body sizes than those of bipeds (1.5 tonnes in bipeds vs. ~4 tonnes, or up to 7 tonnes [15] in Triassic quadrupeds). Nonetheless, *Anchisaurus* (0.26 tonnes) indicates that the smallest quadrupedal sauropodomorphs were similar in mass to the smallest post-Carnian bipeds (*Sarahasaurus*, 0.17 tonnes; see also *Leonerasaurus*). The current phylogenetic position of the inferred bipeds *Mussaurus* and *Yunnanosaurus* suggests the occurrence of at least one reversal back to bipedality. A more detailed understanding of the distribution and evolutionary pattern of quadrupedality is precluded by the lack of reliable

appendicular measurements for several taxa, and especially some of the closest relatives of Sauropoda (e.g., *Lessemsaurus, Ingentia, Leonerasaurus*, *Pulanesaura*), as well as a continued lack of consensus on phylogenetic relationships among non-sauropodan sauropodiforms.

DISCUSSION

Quadrupedality in sauropodomorph dinosaurs

Quadrupedality has been viewed as a key adaptation of Sauropoda, allowing for larger body masses and hence increased gut retention times required for processing low-quality, fibrous vegetable matter [e.g., 18]. Sauropods were unique among quadrupedal dinosaurs in having a columnar stance with erect, parasagittal limbs, allowing efficient, graviportal support of body mass [7, 12, 19], similar to that in large mammals [20]. This is indicated by a set of derived morphological features of sauropod forelimbs, including: reduction of the deltopectoral crest; straightening of the humeral and femoral shafts; the lengthening of the antebrachium and modification of the proximal ulna to a triradiate shape; modification of the metacarpus into a U-shaped support structure; loss of the lesser trochanter, migration of the fourth trochanter distally and medially, increase in fibular robustness; and many others [16, 18]. These features evolved, at least in incipient forms, by the middle of the Early Jurassic, and are exemplified by the early sauropod *Vulcanodon* ([19, 21]; see also *Pulanesaura* [16]).

Unlike sauropods, *Ledumahadi* retains plesiomorphic features of the ulna (i.e., short, robust shaft and a large olecranon process) and femur (i.e., circular shaft, expansive distal condyles). These features are present to some degree in all non-sauropodan sauropodomorphs, and are generally thought to indicate flexed limb postures [6-8, 10, 22] (Figure 4). Flexed (or 'crouched') limb postures are similar to those of smaller-bodied mammals, and distinct from the laterally sprawling limb postures of extant non-avian reptiles. Although a continuum exists between flexed and columnar limb postures, all extant mammals of >300kg body mass have

fully columnar limbs [20], and the same seems to have been true in all sauropods. The presence of even partially flexed forelimbs in *Ledumahadi*, weighing 12 tonnes, is therefore striking, and is consistent with interpretations of other lessemsaurids [15].

Our analysis using linear discriminant functions on limb circumferences finds strong support for quadrupedality in non-sauropodan sauropodiforms, although they lack sauropod-like innovations related to columnar limb postures. The phylogenetic lineage leading to *Ledumahadi* diverged from that of Sauropoda in the Late Triassic (Norian), and its large size (12 tonnes) evolved independently to that of sauropods (Figure 2). The most recent common ancestor of *Ledumahadi* and Sauropoda has an estimated body mass of 2.2 tonnes (Figure 2), and other lessemsaurids, such as *Lessemsaurus* (2.1 tonnes estimated from most complete specimen; although adult body mass likely much larger [15]) and *Antetonitrus* (5.6 tonnes) weighed substantially less than *Ledumahadi*. *Ledumahadi* shows that quadrupedal sauropodomorphs lacking columnar limbs could attain sauropod-like body sizes. This contradicts hypotheses that columnar limb posture enabled multi-tonne masses in sauropods [3, 22].

Ornithischian dinosaurs evolved quadrupedality in several independent lineages, but their osteology shows that none had fully columnar forelimbs [23]. Our findings suggest that early sauropodiforms followed a similar trajectory in the initial adoption of quadrupedality, and that a columnar limb posture evolved only later in one sub-lineage, the sauropods. This columnar limb posture led to a major radiation in Sauropodomorpha.

Previous studies of postural evolution in sauropodomorphs have focused on osteological indicators of manual pronation [e.g., 9, 10]. This is thought to be important as it results in a posteriorly facing hand capable of transmitting force to the ground during locomotion. However, non-sauropodan sauropodiforms have intermediate osteologies indicating incomplete

development of sauropod-like pronation, preventing firm conclusions based on this evidence alone (e.g. [5, 9]). We also note uncertainties in studies of the reconstructed range of motion of dinosaur forelimbs due to the non-preservation of cartilaginous articular surfaces (e.g. [5]). Furthermore, some previously-proposed traits relating to manual pronation (e.g., the ulnar facet on the radius [4]) are of limited utility even across just Dinosauria [23], with recent research suggesting that no dinosaurs could fully pronate the manus [24], unlike mammals. This calls into question the definitiveness of these traits in determining the predominant mode of locomotion during travel, although they clearly do contribute to understanding what a limb is capable of across the range of activities undertaken by an organism. Skeletal correlates of quadrupedality in ornithischian dinosaurs have been more thoroughly explored [23, 25], but even for those, the most reliable inferences depend on the presence of multiple proxy morphologies. Greatest confidence in inferences of quadrupedality should therefore result from indicators that apply universally to independent evolutionary transitions between bipedality and quadrupedality across tetrapods.

Unlike previous approaches, our method is quantitatively validated in a comparative statistical framework, and reliably indicates posture across a broad phylogenetic sample of four-limbed tetrapods. Because it uses simple measurements derived from relatively small portions of the skeleton, we can deploy our method on a wider sample of taxa than in previous studies. Many of our assessments match those made from other evidence (e.g., '*Melanorosaurus*', NMQR 3314 [10]; *Antetonitrus* [4]). Temporally, our findings are also supported by evidence from the ichnological record, which clearly shows quadrupedal sauropodomorphs were present and widely distributed in the Late Triassic [e.g., 26, 27, 28]. The rich ichnofauna of the lower Elliot Formation of western Lesotho includes many quadrupedal sauropodomorph trackways that predate *Ledumahadi*. These were assigned a Late Triassic age by Ellenberger [29], which has been upheld by our ongoing bio- and chronostratigraphic work [30, 31]. Interestingly, when

first described these tracks were presented as evidence for the early occurrence of sauropods [29].

We confirm the hypothesis that quadrupedality preceded the origin of sauropod-like columnar limbs, and was present in sauropodiforms including NMQR 3314 [10] and *Antetonitrus* [8]. However, we differ from previous studies in inferring quadrupedality in earlier-diverging taxa such as *Anchisaurus* and *Jingshanosaurus*, implying a phylogenetically deeper origin that took place at least 15 million years prior to the earliest skeletal evidence of quadrupedal Sauropoda [7, 21]. This has further implications - for example, a previous study suggested that bipedality was primitively retained in *Mussaurus* [9], but we find it instead indicates previously unrecognised homoplasy in the evolution of stance among early sauropodiforms.

Finally, whereas previous work has implied a gradual transition characterised by intermediate, or 'facultative' behaviors [6, 9], we find that most sauropodomorph taxa can be classified unambiguously as either quadrupeds or bipeds, the only exception being *Anchisaurus* (Table S3; 68.9% likelihood of quadrupedality). This suggests that the transition between bipedality and quadrupedality during travel was evolutionarily rapid, with few clear intermediate stages observed in their fossil record so far. This does not preclude a role for the forelimb during foraging or other slow-speed behaviors in otherwise quadrupedal sauropodiforms, and it is possible that *Ledumahadi* represents the maximum size threshold in which a browsing strategy that entailed regular rearing remained viable [7]. Indeed, we find evidence for substantial experimentation in locomotory style among early sauropodomorphs: semi-crouched quadrupedality did not preclude subsequent evolutionary reversals to bipedality (whereas no reversals occur from the columnar-limbed condition of Sauropoda).

Evolution of gigantism in sauropodomorph dinosaurs

Based on current knowledge of the fossil record, *Ledumahadi mafube* was the largest land animal to have ever existed at the time it lived in the earliest Jurassic. It is larger than many sauropods and similar in body mass to the largest ornithischians (12–17 tonnes). The occurrence of *Ledumahadi* shows that, as in ornithischians, columnar forelimb postures were not a prerequisite for massive sizes exceeding 10 tonnes in sauropodomorphs. Nevertheless, columnar forelimbs may be a key structural adaptation allowing body masses far in excess of this seen in some younger sauropods [2] 6]. Recently, a body mass of at least 7 tonnes has been postulated for adult specimens of the Norian taxon *Lessemsaurus*, which is sister to *Antetonitrus* + *Ledumahadi* [15] within the Lessemsauridae. The discovery of *Ledumahadi* indicates a continuous expansion of lessemsaurid body size across the ETE. This indicates either that the maximum body size of giant lessemsaurids was unaffected by the ETE, or rebounded rapidly.

Our findings on *Ledumahadi* provide a striking confirmation of high ecomorphological disparity among earliest Jurassic sauropodomorphs, with a greater disparity of body sizes [2] and postures [31] present than in any other period of sauropodomorph evolution (Figure 2). However, non-sauropodan sauropodomorphs like *Ledumahadi* coexisted for only a short time with columnar-limbed, quadrupedal sauropods like *Vulcanodon*, which by the Toarcian are the only surviving members of the lineage. The reasons for this turnover, and the extinction of non-sauropodan sauropodomorphs, remain unknown. However, at least among large-bodied quadrupeds such as lessemsaurids, it may reflect competitive replacement, facilitated by energy-saving adaptions of the sauropodan forelimb and feeding apparatus [7, 32].

Acknowledgements: The work was made possible by funding provided by the following: the National Research Foundation (NRF) Competitive Programme for Rated Researchers (#98906); the Palaeontological Scientific Trust (PAST) and its Scatterlings of Africa programmes; the DST-NRF Centre of Excellence in Palaeosciences (CoE-Pal); the Friedel Sellschop Award

administered by University of the Witwatersrand; and the Royal Society of London. Parts of this work were funded by the European Union's Horizon 2020 research and innovation programme 2014–2018 under grant agreement 677774 (ERC Starting Grant: TEMPO) to RBJB. BWM is supported by a FAPESP post-doctoral grant to Max Langer. Cynthia Kemp and Celeste Yates prepared all of the fossil material. Viktor Radermacher provided assistance in developing the figures. Portions of the holotype were collected by Sifelani Jirah, James Kitching, Adam Yates, Michael Day, and Alex Parkinson. Puseletso Lecheko provided Sesotho translation for the genus and species name.

AUTHOR CONTRIBUTIONS

BWM conducted fieldwork, collected anatomical, phylogenetic, and measurement data, performed analyses, and co-wrote manuscript.

RBJB collected measurement data, designed experiments, designed and performed analyses, and co-wrote manuscript.

JB-B collected and analysed osteohistological data, funded portions of the study, and co-wrote manuscript

EMB collected and analysed stratigraphic and sedimentological data, funded portions of the study, and co-wrote manuscript

JNC conducted fieldwork, collected anatomical, phylogenetic, and measurement data, performed analyses, funded study, and co-wrote manuscript

Declaration of interests

The authors declare no competing interests.

REFERENCES

1. Benson, R.B.J., Campione, N.E., Carrano, M.T., Mannion, P.D., Sullivan, C., Upchurch, P., and Evans, D.C. (2014). Rates of dinosaur body mass evolution indicate 170 million years of sustained ecological innovation on the avian stem lineage. PLoS ONE *12*, e1001896.
2. Benson, R.B., Hunt, G., Carrano, M.T., and Campione, N. (2017). Cope's rule and the adaptive landscape of dinosaur body size evolution. Palaeontology *61*, 13–48.
3. Sander, P.M., Christian, A., Clauss, M., Fechner, R., Gee, C.T., Griebeler, E.-M., Gunga, H.-C., Hummel, J., Mallison, H., Perry, S.F., et al. (2011). Biology of the sauropod dinosaurs: the evolution of gigantism. Biological Reviews of the Cambridge Philosophical Society *86*, 117-155.
4. Yates, A.M. (2003). A definite prosauropod dinosaur from the Lower Elliot Formation (Norian: Upper Triassic) of South Africa. Palaeontologia africana *39*, 63–68.
5. Otero, A., Allen, V., Pol, D., and Hutchinson, J.R. (2017). Forelimb muscle and joint actions in Archosauria: insights from *Crocodylus johnstoni* (Pseudosuchia) and *Mussaurus patagonicus* (Sauropodomorpha). PeerJ *5*, e3976.
6. Carrano, M.T., Rogers, C., and Wilson, J. (2005). The evolution of sauropod locomotion. The sauropods: evolution and paleobiology. University of California Press, Berkeley, 229-249.
7. McPhee, B.W., Bonnan, M.F., Yates, A.M., Neveling, J., and Choiniere, J.N. (2015). A new basal sauropod from the pre-Toarcian Jurassic of South Africa: evidence of niche partitioning at the sauropodomorph–sauropod boundary? Scientific Reports *5*, 1–12.
8. McPhee, B.W., Yates, A.M., Choiniere, J.N., and Abdala, F. (2014). The complete anatomy and phylogenetic relationships of *Antetonitrus ingenipes* (Sauropodiformes, Dinosauria): implications for the origins of Sauropoda. Zoological Journal of the Linnean Society *171*, 151–205.
9. Yates, A.M., Bonnan, M.F., Neveling, J., Chinsamy, A., and Blackbeard, M.G. (2010). A new transitional sauropodomorph dinosaur from the Early Jurassic of South Africa and the evolution of sauropod feeding and quadrupedalism. Proceedings of the Royal Society of London, Series B *277*, 787–794.
10. Bonnan, M.F., and Yates, A.M. (2007). A new description of the forelimb of the basal sauropodomorph *Melanorosaurus*: implications for the evolution of pronation, manus shape and quadrupedalism in sauropod dinosaurs. Special Papers in Palaeontology *77*, 157-168.
11. Pol, D., and Powell, J. (2007). New information on *Lessemsaurus sauropoides* (Dinosauria: Sauropodomorpha) from the Upper Triassic of Argentina, Volume 77.
12. Allain, R., and Aquesbi, N. (2008). Anatomy and phylogenetic relationships of *Tazoudasaurus naimi* (Dinosauria, Sauropoda) from the late Early Jurassic of Morocco. Geodiversitas *30*, 345-424.
13. Klein, N., and Sander, M. (2008). Ontogenetic stages in the long bone histology of sauropod dinosaurs. Paleobiology *34*, 247-263.
14. Krupandan, E., and Chinsamy-Turan, A. (2018). The long bone histology of the sauropodomorph, *Antetonitrus ingenipes*. The Anatomical Record *in press*.
15. Apaldetti, C., Martínez, R.N., Cerda, I.A., Pol, D., and Alcober, O. (2018). An early trend towards gigantism in Triassic sauropodomorph dinosaurs. Nature Ecology & Evolution.
16. McPhee, B.W., and Choiniere, J.N. (2017). The osteology of *Pulanesaura eocollum*: implications for the inclusivity of Sauropoda (Dinosauria). Zoological Journal of the Linnean Society *182*, 830–861.
17. Campione, N.E., and Evans, D.C. (2012). A universal scaling relationship between body mass and proximal limb bone dimensions in quadrupedal terrestrial tetrapods. BMC Biology *10*, 60.
18. Rauhut, O., Fechner, R., Remes, K., and Reis, K. (2011). How to get big in the Mesozoic: the evolution of the sauropodomorph body plan In Biology of the Sauropod Dinosaurs: Understanding the Life of Giants, N. Klein, K. Remes, C.T. Gee and P.M. Sander, eds. (Bloomington: Indiana University Press), pp. 119–149.

19. Cooper, M.R. (1984). A reassessment of *Vulcanodon karibaensis* Raath (Dinosauria:Saurischia) and the origin of the Sauropoda. Palaeontologia africana *25*, 203–231.
20. Biewener, A.A. (1989). Scaling body support in mammals: limb posture and muscle mechanics. Science *245*, 45-48.
21. Viglietti, P.A., Barrett, P.M., Broderick, T., Munyikwa, D., MacNiven, R., Broderick, L., Chapelle, K., Glynn, D., Edwards, S., Zondo, M., et al. (2018). Stratigraphy of the Vulcanodon type locality and its implications for regional correlations within the Karoo Supergroup. Journal of African Earth Sciences *137*, 149–156.
22. Remes, K. (2008). Evolution of the pectoral girdle and forelimb in Sauropodamorpha (Dinosauria, Saurischia): osteology, myology and function. In Fakultat fur Geowissenschaften, Volume PhD. (Munich: Ludwing Maximilian University of Munich), p. 355.
23. Barrett, P.M., and Maidment, S.C.R. (2017). The evolution of ornithischian quadrupedality. Journal of Iberian Geology *43*, 363-377.
24. Hutson, J.D. (2014). Quadrupedal dinosaurs did not evolve fully pronated forearms: new evidence from the ulna. Acta Palaeontologica Polonica *60*, 599-610.
25. Maidment, S.C.R., and Barrett, P.M. (2014). Osteological correlates for quadrupedality in ornithischian dinosaurs. Acta Palaeontologica Polonica *59*, 53–70.
26. Kent, D.V., and Clemmensen, L.B. (1996). Paleomagnetism and cycle stratigraphy of the Triassic Fleming Fjord and Gipsdalen formations of East Greenland. Bulletin of the Geological Society of Denmark *42*, 121-136.
27. Lallensack, J.N., Klein, H., Milàn, J., Wings, O., Mateus, O., and Clemmensen, L.B. (2017). Sauropodomorph dinosaur trackways from the Fleming Fjord Formation of East Greenland: evidence for Late Triassic sauropods. Acta Palaeontologica Polonica *62*, 833-843.
28. Ellenberger, P. (1972). Contribution á la classification des pistes de vertébrés du Trias: les types du Stormberg d'Afrique du Sud (I), (Montpellier: Laboratoire de paléontologie des vertébrés).
29. Ellenberger, F., Ellenberger, P., and Ginsburg, L. (1967). The appearance and evolution of dinosaurs in the Trias and Lias: a comparison between South African Upper Karoo and western Europe based on vertebrate footprints. In Gondwana Stratigraphy: JUGS Symposium Buenos Aires (Mar del Plata), A.J. Amos, ed. (Buenos Aires (Mar del Plata): UNESCO), pp. 333–354.
30. Bordy, E., Van Gen, J., Tucker, R., and McPhee, B.W. (2015). Maphutseng fossil heritage: stratigraphic context of the dinosaur trackways and bone bed in the Upper Triassic–Lower Jurassic Elliot Formation (Karoo Supergroup, Lesotho). In First International Congress on Continental Ichnology, H. Saber, A. Lagnaoui and A. Belahmira, eds. (El Jadida, Morocco: Chouaïb Doukkali University), p. 67.
31. McPhee, B.W., Bordy, E.M., Sciscio, L., and Choiniere, J.N. (2017). The sauropodomorph biostratigraphy of the Elliot Formation of southern Africa: tracking the evolution of Sauropodomorpha across the Triassic–Jurassic boundary. Acta Palaeontologica Polonica *62*, 441-465.
32. Barrett, P.M., and Upchurch, P. (2005). Sauropodomorph diversity through time: paleoecological and macroevolutionary implications. In The Sauropods: evolution and paleobiology, K.A. Curry Rogers and J.A. Wilson, eds. (Berkeley: University of California Press), pp. 125–136.
33. Duncan, R.A., Hooper, P., Rehacek, J., Marsh, J., and Duncan, A. (1997). The timing and duration of the Karoo igneous event, southern Gondwana. Journal of Geophysical Research: Solid Earth *102*, 18127-18138.
34. Bordy, E.M., Hancox, P.J., and Rubidge, B.S. (2004). Basin development during the deposition of the Elliot Formation (Late Triassic–Early Jurassic), Karoo Supergroup, South Africa. South African Journal of Geology *107*, 397–412.
35. Sciscio, L., de Kock, M., Bordy, E., and Knoll, F. (2017). Magnetostratigraphy across the Triassic-Jurassic boundary in the main Karoo Basin. Gondwana Research *51*, 177-192.

36. Galton, P.M. (1976). Prosauropod dinosaurs (Reptilia: Saurischia) of North America. Postilla *169*, 1-98.
37. Zhang, Y.H., and Zhang, Y.Z. (1994). A new complete osteology of Prosauropoda in Lufeng Basin, Yunnan, China: *Jingshanosaurus*, (Kunming: Yunnan Publishing House of Science and Technology).
38. Otero, A., and Pol, D. (2013). Postcranial anatomy and phylogenetic relationships of *Mussaurus patagonicus* (Dinosauria, Sauropodomorpha). Journal of Vertebrate Paleontology *33*, 1138-1168.
39. Benson, R.B., Campione, N.E., Carrano, M.T., Mannion, P.D., Sullivan, C., Upchurch, P., and Evans, D.C. (2014). Rates of dinosaur body mass evolution indicate 170 million years of sustained ecological innovation on the avian stem lineage. PLoS Biology *12*.
40. Young, C.-C. (1942). *Yunnanosaurus huangi* Young (gen. et sp. nov.), a new Prosauropoda from the Red Beds at Lufeng, Yunnan. Bulletin of the Geological Society of China *22*, 63–104.
41. Maddison, W.P., and Maddison, D.R. (2018). Mesquite: a modular system for evolutionary analysis. 3.40 Edition.
42. Goloboff, P.A., Farris, J.S., and Nixon, K.C. (2008). TNT, a free program for phylogenetic analysis. Cladistics *24*, 774–786.
43. team, R.C. (2013). R: A language and environment for statistical computing. (Vienna: R Foundation for Statistical Computing).
44. Pinheiro, J., Bates, D., DebRoy, S., Sarkar, D., and Team, R.C. (2018). nlme: linear and nonlinear mixed effects models.
45. Paradis, E., Claude, J., and Strimmer, K. (2004). APE: analyses of phylogenetics and evolution in R language. Bioinformatics *20*, 289-290.
46. Venerables, W., and Ripley, B. (2002). Modern applied statistics with S. (new york: Springer).
47. Bapst, D.W. (2012). paleotree: an R package for paleontological and phylogenetic analyses of evolution. Methods in Ecology and Evolution *3*, 803–807.
48. Cerda, I.A., Chinsamy, A., Pol, D., Apaldetti, C., Otero, A., Powell, J.E., and Martínez, R.N. (2017). Novel insight into the origin of the growth dynamics of sauropod dinosaurs. PloS one *12*, e0179707.
49. Stein, K., and Prondvai, E. (2014). Rethinking the nature of fibrolamellar bone: an integrative biological revision of sauropod plexiform bone formation. Biological Reviews *89*, 24-47.
50. Chinsamy, A. (1993). Bone histology and growth trajectory of the prosauropod dinosaur Massospondylus carinatus Owen. Modern Geology *18*, 319-329.
51. Mitchell, J., and Sander, P.M. (2014). The three-front model: a developmental explanation of long bone diaphyseal histology of Sauropoda. Biological Journal of the Linnean Society *112*, 765-781.
52. Sander, P.M., Klein, N., Buffetaut, E., Cuny, G., Suteethorn, V., and Le Loeuff, J. (2004). Adaptive radiation in sauropod dinosaurs: bone histology indicates rapid evolution of giant body size through acceleration. Organisms Diversity & Evolution *4*, 165-173.
53. Krupandan, E., and Chinsamy, A. (2016). The long bone histology of *Antetonitrus ingenipes*: basal Sauropoda and the evolution of the sauropod-type growth strategy. In 19th Biennial Conference of the Palaeontological Society of Southern Africa (Stellenbosch, South Africa).
54. Osborn, H.F., and Mook, C.C. (1919). *Camarasaurus*, *Amphicoelias*, and other sauropods of Cope. Bulletin of the Geological Society of America *30*, 379-388.
55. Novas, F.E. (1996). Dinosaur monophyly. Journal of vertebrate Paleontology *16*, 723-741.
56. Nesbitt, S.J. (2011). The early evolution of archosaurs: relationships and the origin of major clades. Bulletin of the American Museum of Natural History *352*, 1–291.
57. Langer, M.C., and Benton, M.J. (2006). Early dinosaurs: a phylogenetic study. Journal of Systematic Palaeontology *4*, 309-358.

58. Baron, M.G., and Williams, M. (2018). A re-evaluation of the enigmatic dinosauriform *Caseosaurus crosbyensis* from the Late Triassic of Texas, USA and its implications for early dinosaur evolution. Acta Palaeontologica Polonica *63*, 129–145.
59. Apaldetti, C., Martinez, R.N., Alcober, O.A., and Pol, D. (2011). A new basal sauropodomorph (Dinosauria: Saurischia) from Quebrada del Barro Formation (Marayes-El Carrizal Basin), northwestern Argentina. PLoS ONE *6*, e26964.
60. Apaldetti, C., Martinez, R.N., Pol, D., and Souter, T. (2014). Redescription of the skull of *Coloradisaurus brevis* (Dinosauria, Sauropodomorpha) from the Late Triassic Los Colorados Formation of the Ischigualasto-Villa Union Basin, northwestern Argentina. Journal of Vertebrate Paleontology *34*, 1113-1132.
61. McIntosh, J.S. (2005). The genus *Barosaurus* Marsh (Sauropoda, Diplodocidae). Thunder Lizards: the Sauropodomorph Dinosaurs. Indiana University Press, Bloomington, Indiana, 38-77.
62. Remes, K. (2006). Revision of the Tendaguru sauropod dinosaur *Tornieria africana* (Fraas) and its relevance for sauropod paleobiogeography. Journal of Vertebrate Paleontology *26*, 651-669.
63. Janensch, W. (1961). Die gliedmaßen und gliedmaßengürtel der Sauropoden der Tendaguru-Schichten. Palaeontographica-Supplementbände, 177-235.
64. Canudo, J.I., Royo-Torres, R., and Cuenca-Bescós, G. (2008). A new sauropod: Tastavinsaurus sanzi gen. et sp. nov. from the Early Cretaceous (Aptian) of Spain. Journal of Vertebrate Paleontology *28*, 712-731.
65. Garland, J., Theodore, and Ives, A.R. (2000). Using the past to predict the present: confidence intervals for regression equations in phylogenetic comparative methods. The American Naturalist *155*, 346-364.
66. Burnham, K.P., and Anderson, D.R. (2004). Multimodel inference: understanding AIC and BIC in model selection. Sociological methods & research *33*, 261-304.
67. Campione, N.E., Evans, D.C., Brown, C.M., and Carrano, M.T. (2014). Body mass estimation in non-avian bipeds using a theoretical conversion to quadruped stylopodial proportions. Methods in Ecology and Evolution *5*, 913-923.
68. Sereno, P. (1999). The evolution of dinosaurs. Science *284*, 2137–2147.
69. Chinnery, B. (2004). Morphometric analysis of evolutionary trends in the ceratopsian postcranial skeleton. Journal of Vertebrate Paleontology *24*, 591-609.
70. Galton, P.M. (1970). The posture of hadrosaurian dinosaurs. Journal of Paleontology, 464-473.
71. Maidment, S.C., and Barrett, P.M. (2012). Osteological correlates for quadrupedality in ornithischian dinosaurs. Acta Palaeontologica Polonica *59*, 53-70.
72. Bonnan, M.F. (2007). Were the basal sauropodomorph dinosaurs *Plateosaurus* and *Massospondylus* habitual quadrupeds? Evolution and palaeobiology of early sauropodomorph dinosaurs, 139-155.
73. Mallison, H. (2010). The digital *Plateosaurus* II: an assessment of the range of motion of the limbs and vertebral column and of previous reconstructions using a digital skeletal mount. Acta Palaeontologica Polonica *55*, 433-458.
74. Bonnan, M.F. (2003). The evolution of manus shape in sauropod dinosaurs: implications for functional morphology, forelimb orientation and phylogeny. Journal of Vertebrate Paleontology *23*, 595–613.
75. McPhee, B.W., and Choiniere, J.N. (2016). A hyper-robust sauropodomorph dinosaur ilium from the Upper Triassic–Lower Jurassic Elliot Formation of South Africa: Implications for the functional diversity of basal Sauropodomorpha. Journal of African Earth Sciences *123*, 177-184.
76. Galton, P.M. (1974). Notes on *Thescelosaurus*, a conservative ornithopod dinosaur from the Upper Cretaceous of North America, with comments on ornithopod classification. Journal of Paleontology, 1048-1067.
77. Mallison, H. (2010). The digital *Plateosaurus* I: body mass, mass distribution, and posture assessed using CAD and CAE on a digitally mounted complete skeleton. Palaeontologia Electronica *13*.

78. Marsh, O.C. (1891). I.—Restoration of *Stegosaurus*. Geological Magazine *8*, 385-387.
79. Grafen, A. (1989). The phylogenetic regression. Phil. Trans. R. Soc. Lond. B *326*, 119-157.
80. Cooper, M.R. (1981). The prosauropod dinosaur *Massospondylus carinatus* from Zimbabwe: its biology, mode of life, and phylogenetic significance. Occasional Papers of the Natural History Museum of Rhodesia, Series B: Natural Sciences *6*, 689–840.
81. Ibrahim, N., Sereno, P.C., Dal Sasso, C., Maganuco, S., Fabbri, M., Martill, D.M., Zouhri, S., Myhrvold, N., and Iurino, D.A. (2014). Semiaquatic adaptations in a giant predatory dinosaur. Science *345*, 1613-1616.
82. Pagel, M. (1999). The maximum likelihood approach to reconstructing ancestral character states of discrete characters on phylogenies. Systematic biology *48*, 612-622.
83. Lockley, M.G., and Wright, J.L. (2001). Trackways of large quadrupedal ornithopods from the Cretaceous: a review. Mesozoic vertebrate life, 428-442.
84. McPhee, B.W., Choiniere, J.N., Yates, A.M., and Viglietti, P.A. (2015). A second species of Eucnemesaurus Van Hoepen, 1920 (Dinosauria, Sauropodomorpha): new information on the diversity and evolution of the sauropodomorph fauna of South Africa's lower Elliot Formation (latest Triassic). Journal of Vertebrate Paleontology *36*, e980504.
85. Sertich, J.J., and Loewen, M.A. (2010). A new basal sauropodomorph dinosaur from the Lower Jurassic Navajo Sandstone of southern Utah. PLoS One *5*, e9789.
86. Galton, P.M., and Van Heerden, J. (1985). Partial hindlimb of *Blikanasaurus cromptoni* n. gen. and n. sp., representing a new family of prosauropod dinosaurs from the Upper Triassic of South Africa. Geobios *18*, 509-516.

Figures

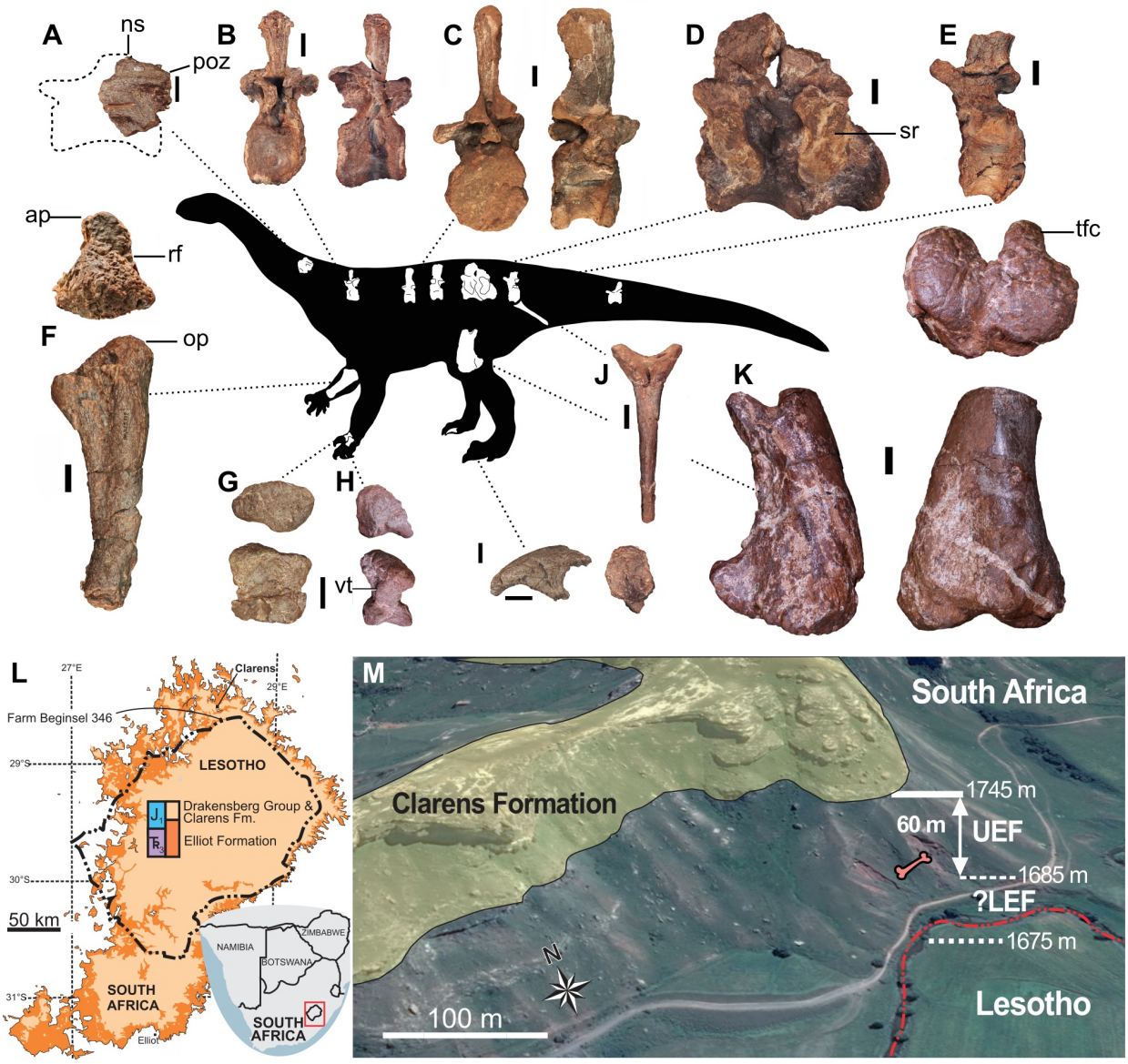

Figure 1. Selected preserved elements of *Ledumahadi mafube* (BP/1/7120), and geography and stratigraphy of type locality: (**A**), middle/posterior cervical vertebra in left lateral view; (**B**), anterior dorsal vertebra in anterior and right lateral views; (**C**), middle dorsal vertebra in posterior and right lateral views; (**C**), first and second 'primordial' sacral vertebrae in left lateral view; (**E**), anterior caudal vertebra in left lateral view; (**F**), right ulna in proximal and medial views; (**G**), first metacarpal in proximal and ?dorsal/ventral views; (**H**), left ?third metacarpal in proximal and ventral views; (**I**), pedal ungual in ?lateral and proximal views; (**J**), anterior chevron in posterior view; (**K**), distal right femur in distal, lateral, and anterior views; (**L**), simplified geological map of the Elliot Formation in the Republic of South Africa and Lesotho

indicating the location of farm Beginsel 346 and aerial extent of the Elliot Formation outcrop area (map modified after the 1:1000000 Geological map of RSA and Lesotho 1984); (**M**), landscape view of the local geology at the Ledumahadi site. Note that the contact of the lower and upper Elliot Formations (LEF/UEF) has been identified at 1685 m above sea level, thus the UEF is ~60 m thick. The poorly exposed LEF, which is ~10 m thick here, only contains massive mudstones with very weakly developed pedogenic alteration features, green-gray mottles, and very rare desiccation cracks. Abbreviations: ap, anterior process; ns, neural spine; op, olecranon process; poz, postzygapophysis; rf, radial fossa; sr, sacral rib; tfc, tibiofibular crest; vt, ventral tubercle. All scale bars equal 5cm. See also Figures S1, S2, Data S1.

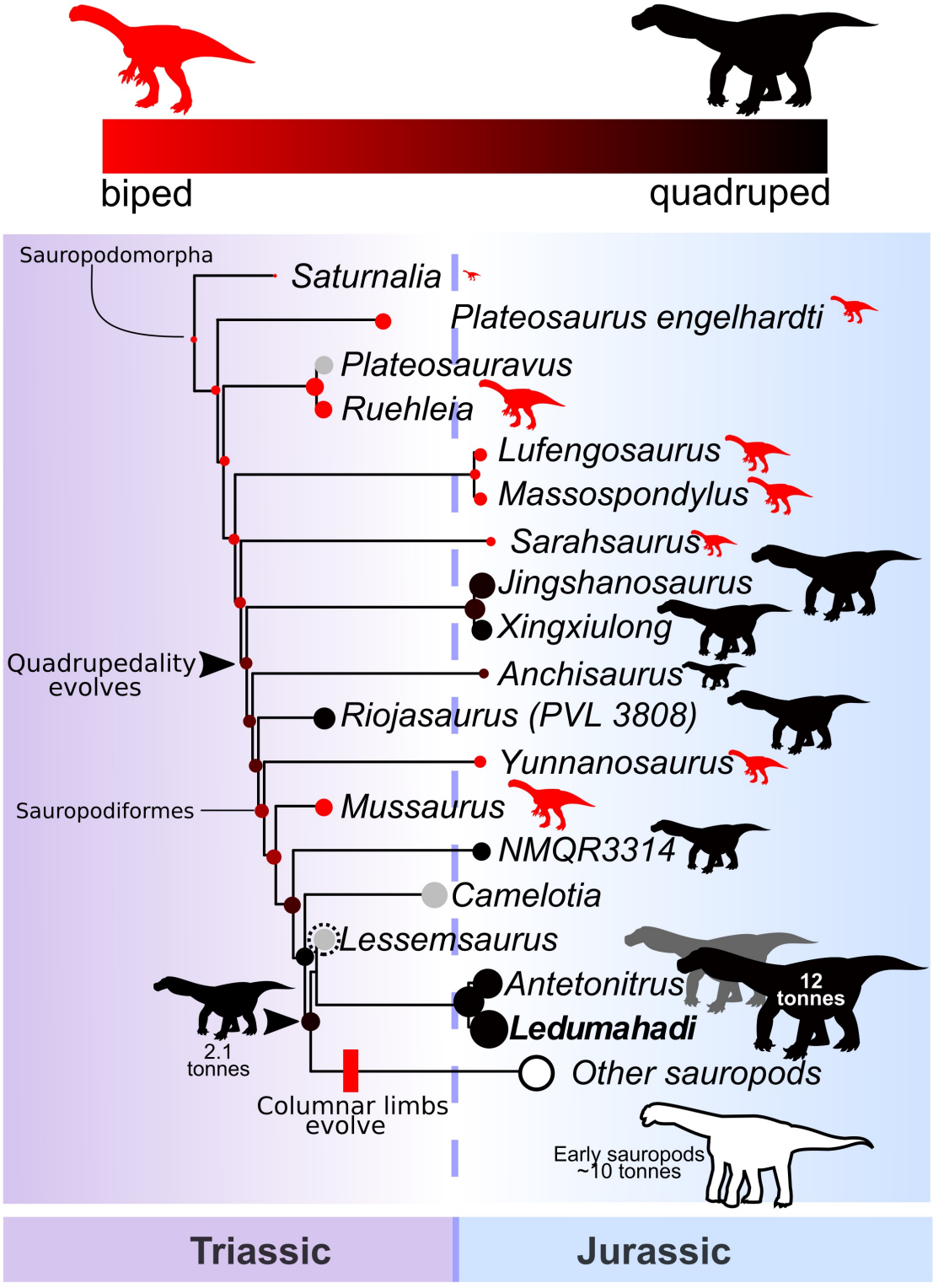
biped
quadruped
Sauropodomorpha
Saturnalia
Plateosaurus engelhardti
Plateosauravus
Ruehleia
Lufengosaurus
Massospondylus
Sarahsaurus
Jingshanosaurus
Xingxiulong
Quadrupedality evolves
Anchisaurus
Riojasaurus (PVL 3808)
Yunnanosaurus
Sauropodiformes
Mussaurus
NMQR3314
Camelotia
Lessemsaurus
Antetonitrus
Ledumahadi
12 tonnes
2.1 tonnes
Other sauropods
Columnar limbs evolve
Early sauropods ~10 tonnes
Triassic
Jurassic

Figure 2. Summarized results of phylogenetic analysis (restricted to taxa with relevant posture and mass data; for strict consensus tree see Figure S4) and linear discriminant function analysis of posture. Diameter of circles scaled to cube root of mass estimate of the taxon. Silhouettes are scaled in height to cube root of mass estimate of the taxon. Grey circles represent absence of locomotory inference. Colour of silhouettes represents inferred posture: red is bipedal and black is quadrupedal. Open circle and silhouette represents members of Sauropoda, where posture is inferred to be quadrupedal but columnar rather than flexed. Dashed purple line marks Triassic/Jurassic boundary. Dashed open circle represents possible adult body mass of *Lessemsaurus*, after [15]. Key inferences of postural evolution marked by arrows and bars. Select taxonomic names indicated. See also Figures S1, S3, S4, Data S1, and STAR Methods for postural inference and body mass.

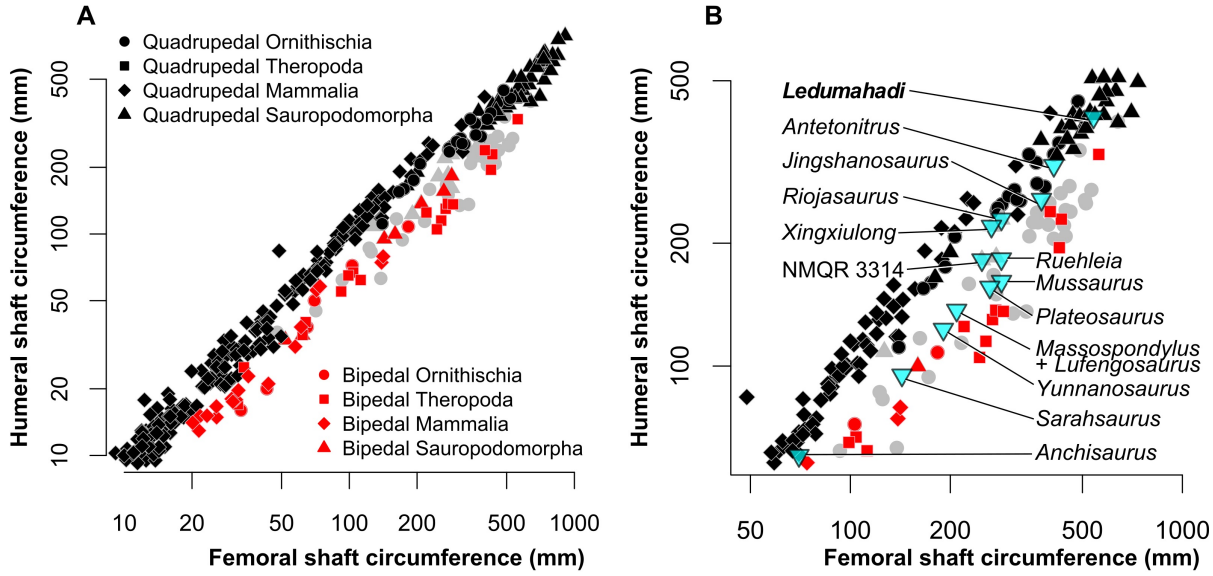

Figure 3. Relationship between (log_{10}-transformed) humeral minimum shaft circumference and femoral minimum shaft circumference in dinosaurs, mammals, and extant reptiles/amphibians [N = 423]. In (**A**), data for all tetrapods including mammals, dinosaurs, and extant

reptiles/amphibians [N = 423]; (**B**), magnified region highlighting transitional sauropodomorphs of uncertain stance (blue inverted triangles). Diamonds = mammals, circles = ornithischian dinosaurs, squares = theropod dinosaurs, triangles = sauropodomorph dinosaurs. Red points = bipeds, black points = quadrupeds, grey points = extinct taxa with uncertain stance, blue inverted triangles = transitional sauropodomorphs of interest for this study (labelled with genus names). See also Figures S1–S3, STAR Methods.

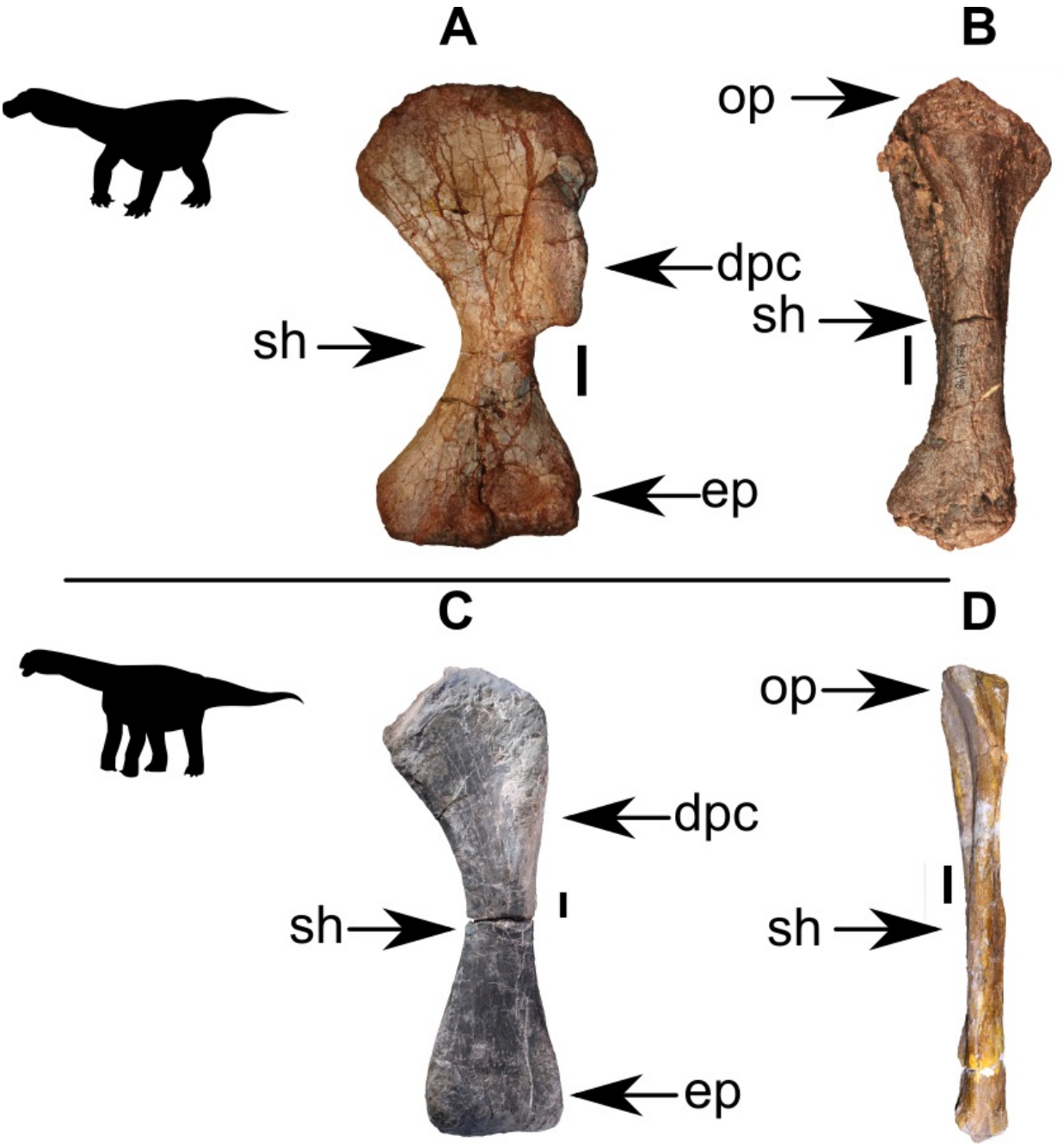

Figure 4. Differences in forelimb morphology between flexed-limbed and columnar-limbed quadrupedal sauropodomorphs. Note especially differences in the size of the deltopectoral crest (dpc), proportional robusticity of the shaft (sh), size of the olecranon process (op), and expansion of the epiphyses (ep). In (**A, B**): forelimb elements of flex-limbed sauropodomorphs: (**A**), left humerus of *Riojasaurus*; (**B**), right ulna (reversed) of *Ledumahadi*. In (**C, D**): forelimb elements of columnar-limbed sauropodomorphs: (**C**) left humerus of *Tazoudasaurus*; (**D**) right

ulna (reversed) of *Vulcanodon*. All bones in anterior view. Silhouettes indicate limb postures and are not to scale. All scale bars equal 5cm.

STAR METHODS

CONTACT FOR REAGENT AND RESOURCE SHARING

Further information and requests for resources and reagents should be directed to and will be fulfilled by the Lead Contact, Jonah Choiniere (jonah.choiniere@wits.ac.za).

EXPERIMENTAL MODEL AND SUBJECT DETAILS

Repository of type specimen

The holotype of *Ledumahadi mafube* (BP/1/7120) and all osteohistological slides are housed at the Evolutionary Studies Institute, University of the Witwatersrand, Johannesburg, South Africa.

Geological context for type specimen

The vicinity of the *Ledumahadi* type locality on Beginsel farm is dominated by the continental sedimentary rocks of the Molteno, Elliot and Clarens formations (Upper Triassic to Lower Jurassic Stormberg Group) as well as the 183±1.0 Ma old intrusive and extrusive mafic rocks of the Drakensberg Group [33] (Figures 1, S1). The Upper Triassic-Lower Jurassic Elliot Formation is a fluvio-lacustrine unit and has an unconformable, sharp, regionally traceable contact with the fluvio-lacustrine and coal-bearing Molteno Formation and a conformable, chiefly gradational contact with the mainly aeolian Clarens Formation [34].

At the *Ledumahadi* type locality, the lower contact of the host Elliot Formation is not exposed, however <3 km to the west (at 28°37'19.39"S; 28°24'40.97"E), the entire thickness of the Elliot

Formation is accessible over a vertical distance of ~200 m. If the lower contact is an even, horizontal surface, the minimum thickness of the Elliot Formation at the *Ledumahadi* site is ~75 m. Stratigraphically, the *in situ Ledumahadi* material was recovered ~45 m below the base of the Clarens Formation (Figures 1, S1). The stratigraphic positioning of the *Ledumahadi* material within the upper Elliot Formation is not only based on its relative proximity to the base of the Clarens Formation but, more importantly, on the sedimentary facies characteristics of the host silty mudrocks (Figure S1).

Although not all diagnostic features of the upper Elliot Formation (e.g., the unique carbonate nodule conglomerate; laterally persistent, sheet-like sandstone units) are present at the *Ledumahadi* site, the available sedimentological record is compelling for an upper Elliot Formation stratigraphic positioning of the *Ledumahadi* material. These features (Figure S1) include the frequent pedogenic alteration of the deep red, maroon to deep pink host rocks (e.g., *in situ* carbonate nodules, root traces, invertebrate traces), as well as the presence of some typical sedimentary facies of the upper Elliot Formation (e.g., clast-rich sandstones: facies Sc, see Figure S1). Taken together, the sedimentary facies association at the *Ledumahadi* type locality (Figure S1) suggests that the sediments were deposited in a vegetated floodplain environment in an overall semi-arid climate. Evidence for increasingly well-drained soils and higher energy depositional conditions (Figure S1: G-M) towards the upper part of the recorded succession may suggest that the floodplain environment was positioned progressively more proximal to some larger river channels. The earliest Jurassic (Hettangian–Sinemurian) age of the upper Elliot Formation at *Ledumahadi* site is inferred from regional magneto- and biostratigraphic investigations as summarized by [35] and [31].

Data sources for transitional sauropodomorphs

Anchisaurus polyzelus, based on YPM 1883 [36] for humeral and femoral circumference comparison. The shaft circumferences were estimated from anteroposterior and mediolateral diameters (femur; circumference estimate = 70 mm) and from mediolateral diameter (humerus; estimated to be 60 mm from mediolateral shaft diameter using equation 17 of Benson et al. 2017, appendix). The body mass of *Anchisaurus* was estimated using data from a larger individual (YPM 208; FC = 126 mm; humerus unknown), scaled to the proportional humerus circumference of YPM 1883.

Antetronitrus ingenipes was measured directly from BP/1/4952.

Jingshanosaurus xinwaensis, based on LV 003 [37], using anteroposterior and mediolateral shaft diameters to estimate shaft circumferences.

Mussaurus patagonicus based on MLP 68-II-27-1 [38], using anteroposterior and mediolateral shaft diameters to estimate shaft circumferences.

NMQR 3314 is a referred specimen of *Melanorosaurus* that was measured directly.

Riojasaurus incertus, based on the holotype and largest individual, PVL 3808 using direct measurements of HC and FC from [2, 39].

Yunnanosaurus huangi, based on IVPP V20 [40], using anteroposterior and mediolateral shaft diameters to estimate shaft circumferences.

KEY RESOURCES TABLE

METHOD DETAILS

The specimen was consolidated in the field using Paraloid B-76 copolymer resin dissolved in acetone. It was excavated using standard field techniques (e.g., plaster and burlap jacket to protect specimen). Removal of rock matrix from fossil bone was done by hand using Palaeotools Mighty Jack and Microjack airscribes. Measurements of all specimens in this

analysis were collected using digital sliding calipers. Phylogenetic data were assembled in Mesquite v3.40 (and lower versions; [41]) and analysed under the parsimony criterion in TNT [42].

QUANTIFICATION AND STATISTICAL ANALYSIS

Our statistical analyses were conducted in R version 3.1.0 [43] using functions available in the packages nlme 3.1-131 [44], ape 4.1 [45], MASS [46], and paleotree 2.3 [47]. Significance of phylogenetic generalised least squares regressions was determined using inbuilt t-statistics in nlme [44].

Osteohistological analysis

The anatomical positions where histological data were collected are shown in Figure S2, and a list of slides with accession numbers is available via the Key Resources Table. The bone tissues of BP/1/7120 show that this individual deposited rapidly forming fibrolamellar bone through much of ontogeny, transitioning to slower growing lamellar-zonal bone later in life (Figure S2: A, B). Much of the primary bone tissue of the inner half of the cortex of the specimen has been destroyed by secondary remodeling (resorption front, rf in Figure S2: A). The middle cortex contains mostly primary fibrolamellar bone with scattered smaller resorption cavities and secondary osteons, thereafter resorption cavities are more restricted (Figure S2: C). Some areas in this region have longitudinally-oriented primary osteons and reticular vascular arrangements, but most canals are arranged in a plexiform to laminar network (Figure S2: C, E). The bands of alternating reticular and plexiform vascular arrangements seen in the closely related sauropodiform *Lessemsaurus* [48] were not observed, but only part of the anterior region was thin-sectioned, and it is possible that other parts of the midshaft may have exhibited such bands.

The patches of primary bone tissue still present in the inner cortex contain a woven-fibered interstitial matrix with abundant globular osteocyte lacunae (Figure S3:D, F). In the middle to outer cortex the lamellae surrounding the primary osteons are substantially thicker and frequently contact one another, giving the bone tissue a parallel-fibered appearance with very little interstitial woven-fibered bone between the lamellae [49]. The outermost cortex becomes increasingly lamellar with highly organized flattened osteocyte lacunae. Narrow annuli of avascular lamellar bone, indicating a temporary decrease in growth rate, appear in the outer 40% of the compact cortex (Figure S2: A, C). It is not known if growth marks only appear during mid-late ontogeny as in the more derived sauropods [13], or if *Ledumahadi* expressed growth marks from early ontogeny similar to the more basal non-sauropodan Sauropodomorpha [49]. Much of the primary tissues in the innermost cortex have been resorbed by secondary remodeling. Fourteen to fifteen growth marks were counted (Figure S2: A), but a large crack in the outer third of the cortex and subsequent fragmentary nature of the bone in this area, as well as the innermost cortical remodeling precludes a definitive count. Lines of Arrested Growth (LAGs), indicating a temporary cessation in growth, begin to appear with numerous annuli within the outermost peripheral lamellar bone. The LAGs are double or triple in places and become increasingly closely spaced indicating a substantial decrease in growth rate. Vascular canals separate these outer growth marks and are present at the outermost periphery indicating that the animal was still growing, but the amount of bone deposition between each growth mark is negligible compared to the earlier growth. Thus, we consider the peripheral lamellar-zonal bone to be an External Fundamental System (EFS) where maximum size had essentially been reached, indicating that this individual was an adult at the time of death. The lamellar infilling of the vascular canals, degree of remodeling and abundance of secondary osteons, as well as the presence of an EFS suggest that the bone tissues fall within the Type E to Type F categories of [13] and Histologic Ontogenetic Stage 10 or 11. Extensive Sharpey's fibers, indicating areas for

the probable attachment of the femorotibialis muscles, were found all along the bone periphery, but also extend as thick bundles a third of the way into the cortex. A few remnants are even present in the inner cortex. The Sharpey's fiber bundles are frequently associated with radially-oriented vascular canals.

Although all sauropodomorph bone tissues studied thus far exhibit rapidly forming woven-fibered bone during early ontogeny, non-sauropodan sauropodomorph bone tissues such as those of *Plateosaurus* and Massospondylidae tend to exhibit a predominance of the relatively slower forming parallel-fibered bone during mid-late ontogeny [13, 48]. The bone tissues of these taxa are also interrupted by regularly spaced LAGs even during early ontogeny [13, 50]. This differs from more derived Late Jurassic Neosauropoda, which typically exhibit uninterrupted laminar fibrolamellar bone until late ontogeny, when the transition to slowly forming lamellar-zonal bone with clear LAGs indicates a dramatic decrease in overall growth rate [51]. The lack of growth marks throughout much of sauropod ontogeny is thought to be due to the selection for rapid growth rates in order to reach their enormous body sizes [51, 52]. The presence of uninterrupted fibrolamellar bone even in the possibly Late Triassic basal sauropod *Isanosaurus* suggests that growth acceleration occurred very early in sauropod evolutionary history [52].

Although *Isanosaurus* shows that the earliest sauropods were capable of sustained growth, late branching non-sauropodan sauropodiforms such as *Lessemsaurus* [48] and *Antetonitrus* [53] exhibit growth marks during early ontogeny. Although early cyclical growth cannot be confirmed in *Ledumahadi* (due to the resorption of the earliest growth), the presence of growth marks from at least 60% through ontogeny suggests that it grew similarly to these other non-sauropodan sauropodiforms. Interestingly, the first few annuli are not associated with LAGs indicating that growth slowed, but did not cease completely, contrary to that observed in other non-sauropodan Sauropodomorpha, including *Lessemsaurus* [48] and suggests higher growth

rates during the unfavorable growing season. Thus, the bone tissues of *Ledumahadi* contain aspects of non-sauropodan sauropodomorph and more derived sauropod life histories, emphasizing the variability characterizing sauropodiform osteohistology during a period of heightened ecological diversification.

Phylogenetic analysis

To assess the relationships of the holotype of *Ledumahadi*, we scored it using the phylogenetic dataset of [16], which is based on the original dataset of [9]. We added the following two characters:

Ch. 218: Anterior tip of anterior process of proximal ulna: no deflection or continues lateral curvature (0); medially deflected (1).

A medially deflected anterior process of the ulna was originally described as an autapomorphy of *Antetonitrus* [8]. However, as a similar deflection is observed in *Ledumahadi*, this feature was added to the dataset as a possible synapomorphy of the two taxa.

Ch. 233: Pronounced tubercle on the ventrolateral corner of the shaft of the non-first metacarpals, just below the proximal surface: absent (0); present (1).

This character extends from observations made in [8], in which the presence of a pronounced tubercle on the ventrolateral corner of the shaft was used to side the second metacarpal in *Antetonitrus*. A large, topographically similar process is observed in the only non-first metacarpal currently known for *Ledumahadi* (which is possibly a third or fourth based on size comparison with the first metacarpal). Although the lack of well-preserved hands in many sauropodomorph taxa precludes a deeper understanding of the polarity of this character (as well as its manifestation across the metacarpus), current observations suggest that it typifies a group of robust-limbed sauropodiforms, *Ledumahadi* and *Antetonitrus* included.

An additional state was also added to ch. 204 (transverse width of the distal condyles of the humerus): (2) 40 percent or more of the length of the humerus (unordered). This was based on the observation that the humerus of some sauropodomorph taxa (e.g., *Riojasaurus*, *Yunnanosaurus*, *Lessemsaurus*) presents apomorphically widened distal condyles.

The following two characters were removed from the dataset:

Sacral rib much narrower than the transverse process of the first primordial sacral vertebra (and dorsosacral if present) in dorsal view: absent (0); present (1).

This character was removed on grounds of both difficulty of interpretation, as well as presenting a conflation of two distinct morphologies (the dorsosacral and first primordial sacral vertebrae). In most basal sauropodomorph taxa with three sacral vertebrae (e.g., *Adeopapposaurus*; *Lufengosaurus*), the transverse process and sacral rib of the first element combine to form a large 'C'-shaped attachment with the ilium, with the majority of the anterior and ventral sections of the 'C' comprised of the sacral rib. In contrast, the second sacral element often bears a more 'hourglass' shaped iliac attachment in which the dorsal transverse process and ventral rib are roughly equivalent in anteroposterior width. Together, the sacral ribs of the conjoined pelvic vertebrae tend to form a continuous shelf that borders the mediodorsal margin of the iliac acetabulum – meaning that, if anything, the sacral ribs are uniformly more expansive than the transverse processes across all sauropodomorph taxa (including sauropods, e.g., *Camarasaurus* [54; fig. 44]). This situation potentially applies to dinosaurs in general (e.g., [55]: Figure 7).

A further issue pertains to the identity of the first two sacral elements. Whereas the first sacral vertebra in a three-sacral arrangement is often considered to represent a dorsosacral, its anatomy is generally much closer to that of the first primordial sacral vertebra in taxa for which only two sacral elements are present (e.g., *Herrerasaurus*, *Efraasia*). In contrast, the middle element (the

'first primordial sacral') displays a relatively novel morphology. This was first observed by Nesbitt [56], who interpreted the middle element as a novel insertion between the two primordial sacral vertebrae – rendering the traditional 'dorsosacral' of recent sauropodomorph studies the first primordial sacral. It is this interpretation that is considered the most likely here. Further analysis of these morphologies and their distribution across sauropodomorphs (and other dinosaur taxa) is required prior to its re-inclusion in the dataset (see [4, 56, 57] for further comment).

Buttress between preacetabular process and the supraacetabular crest of the ilium: present (0) or absent (1).

This character was scored seemingly randomly across the taxa in the dataset. However, a distinct buttress such as described here is not observable in any dinosaurian taxon. In contrast, some crurotarsan taxa display a pronounced ridge that connects the iliac supraacetabular crest to the anterior portion of the dorsal iliac blade (e.g., *Postosuchus*). If restricted to its actual distribution, the 'present' state of this character could only be scored polymorphically for one taxon (Crurotarsi) in the current dataset (i.e., is parsimony uninformative). Recently, Baron and Williams [58] noted that a number of dinosauriform taxa have at least a rounded eminence connecting the dorsal surface of the acetabulum to the ventral surface of the preacetabular process – with this feature more pronounced in silesaurid and herrerasaurid dinosauromorphs. However, the degree to which this feature can be considered a distinct buttress remains open to interpretation.

We managed the phylogenetic dataset in Mesquite v3.40 [41], and exported character/state information to TNT [42] for analysis under the parsimony criterion. A nexus file containing our matrix is available via the key resources table of this publication. We searched for optimal trees using 1000 Wagner additions, holding 1 tree per replicate and swapping on topologies using

Tree Bisection and Reconnection. The final set of trees under this analysis was then subjected to another round of TBR searching, up to a maximum of 10,000 final topologies. The following multistate characters were treated as ordered: 8, 13, 19, 23, 40, 57, 69, 92, 102, 117, 121, 131, 134, 145, 148, 150, 151, 158, 163, 168, 171, 177, 184, 207, 210, 217, 226, 231, 239, 247, 255, 258, 271, 283, 304, 310, 318, 338, 351, 354, 356, 361, 365.

This analysis resulted in 6 MPTs with a shortest length of 1286 steps (CI: 0.338; RI: 0.688). All trees found *Ledumahadi* to be the sister taxon to the upper Elliot taxon *Antetonitrus ingenipes*, a position supported by a Bremer value of 2 and the following unambiguous synapomorphies: dorsoventral height of mid-dorsal neural spines over 1.5 times the anteroposterior length of their base (ch. 168); presence of well-developed spinopostzygapophyseal laminae in posterior dorsal vertebrae (ch. 172); anterior tip of the anterior process of the proximal ulna deflected medially (ch. 218). Overall, the strict consensus topology (Figure S4) is somewhat different from previous topologies (e.g, [7, 38, 59]). Of interest is the non-massospondylid position of *Coloradisaurus* and *Glacialisaurus*, which is undoubtedly a reflection of the numerous plateosaur-like features of the former (especially in regards to the cranial anatomy), a concern treated in detail in [60]. Additionally, restriction of the character scorings for *Riojasaurus* to those observable in the holotype (PVL 3808) appears to have introduced renewed instability to this part of the sauropodomorph tree, with the sauropodiform position of this specimen (based primarily on its derived appendicular proportions) only a marginally better explanation than a position closer to *Plateosauravus*, with which it shares several features (e.g., heel on the posteroventral corner of the iliac ischial peduncle). This is reflected in the bootstrap re-sampling analysis, in which relationships amongst ‘core prosauropods’ are unresolved at frequencies greater than 50% (Figure S4).

It is clear, therefore, that the major interrelationships of basal sauropodomorph dinosaurs remain far from conclusively settled.

Body mass estimates of *Ledumahadi mafube*

We used measurements taken from a published database [39] and from personal research by the authors and regression equations taken from [17] to estimate the body mass of *Ledumahadi mafube* from measurements of the preserved limb bones, which include the femur (minimum shaft circumference = 540 mm) and ulna (total length = 490 mm; minimum shaft circumference = 265 mm). Our minimum diameter was taken approximately 10cm proximal to the proximal end of the popliteal fossa, exactly at the same point where the femur of *Antetonitrus* attains its minimum circumference. Therefore, our measurement likely reflects the true minimum circumference of the shaft.

The minimum circumference of the femoral shaft of *Ledumahadi mafube* is only slightly smaller than that of *Tyrannosaurus rex* (RSMP 2523.8; = 570 mm), which is the largest-known bipedal dinosaur with an estimated body mass of 7.69 tonnes. Among quadrupedal sauropodomorphs, it is similar to the dimensions of *Barosaurus lentus* (540 mm; 13.2 tonnes; [61]; AMNH 6341), *Tornieria africana* (545 mm; 12.3 tonnes; [62]; SMNS 12140, right femur of holotype 'skeleton A' of [63]; and *Tastavinsaurus sanzi* (550 mm; 14.0 tonnes; [64]) (body masses from [2, 39]). These comparisons demonstrate that *Ledumahadi* is comparable in size to many sauropods, and therefore much larger than the largest other non-sauropodan sauropodomorphs, which have considerably smaller skeletal dimensions. For example, the minimum femoral shaft circumference of *Antetonitrus* is 410 mm, comparable to *Loxodonta africana* in the dataset of [17; minimum femoral shaft circumference = 399 mm].

To estimate the body mass of *Ledumahadi mafube* using the method of [17] we required an estimate of the minimum circumferences of both the humeral and femoral shafts. Although the femur is preserved, and could be measured directly, the humerus is not known. To establish a

predictive framework for estimating humeral shaft circumference from ulnar shaft circumference, we used the set of 18 Triassic–Cretaceous sauropodomorphs that were present in our phylogeny, and for which both the ulna and humeral minimum shaft circumferences were known. We compared ordinary and phylogenetic generalized least squares linear models of the relationship between $\log_{10}$-transformed humeral shaft circumference and ulnar shaft circumference for these taxa. Phylogenetic generalized least squares (assuming Brownian motion-like evolution of the relationship between variables) is mathematically analogous to ordinary least squares regression of independent contrasts [65] and was implemented using the R packages ape version 4.1 and nlme version 3.1-131; [44, 45].

Akaike's information criterion for finite sample sizes (AICc; see [66]) favours ordinary least squares (AICc = -37.4) over pGLS (AICc = -35.0), similar to most scaling relationships between limb bones in other dinosaur groups [2]. This relationship explains an extremely high proportion of the variance in the relationship between the variables ($R^2 = 0.977$), and suggests a constrained relationship between the robustness of the ulna and that of the humerus in sauropodomorph dinosaurs (Figure S3). The OLS model provides an estimate of 408 mm for the minimum shaft circumference of the humerus of *Ledumahadi mafube*, with upper and lower 95% confidence intervals of 381 mm and 436 mm.

Using the OLS scaling relationship of [17] for quadrupedal dinosaurs, the central tendency of our humeral minimum shaft circumference estimate provides a mass estimate of 12.0 tonnes for *Ledumahadi mafube*. If the humeral minimum shaft circumference were confidently known then this would yield narrower confidence intervals (±2 standard deviations: 6.42–22.4 tonnes). However, it is estimated from the ulnar shaft circumference, and propagation of this error through two rounds of regression results in wider confidence intervals (3.46–41.6 tonnes; using scripts provided by [2]). Regardless of how these confidence intervals are interpreted,

Ledumahadi has skeletal dimensions similar to sauropods with similar femoral shaft circumferences described above, and much greater than those of other sauropodomorphs.

If *Ledumahadi mafube* were assumed to be an habitual biped (an assumption that we strongly reject based on linear discriminant analysis; described below), its body mass would be estimated as 6.63 tonnes (3.55 tonnes – 12.4 tonnes) using the scaling relationship for estimation of the body mass of bipedal tetrapods using femoral shaft circumference provided by [67].

Analysis of terrestrial vertebrate limb-scaling dynamics

Quadrupedality evolved from bipedal ancestors at least three times independently among dinosaurs, in sauropods, ceratopsians and thyreophorans (stegosaurs and ankylosaurs) [19, 23, 68, 69]. Further origins of quadrupedality may also be present in iguanodontians [70, 71], although this remains uncertain. Inferring the presence of quadrupedality in some dinosaurs, and especially 'transitional' taxa such as non-sauropodan sauropodomorphs is difficult [8, 10, 72, 73], leading to a significant lack of consensus about the locomotory status of key taxa. Previous attempts to infer quadrupedality in dinosaurs have focussed on the inference of limb myology and kinematics, as well as the use of discrete character observations as osteological correlates, and have not yet decisively addressed this question ([4, 7-9, 22, 74, 75].

We propose a new method for inferring the number of limbs involved in locomotion that makes use of the robustness of the humeral shaft, captured by a measurement of its minimum circumference, in comparison to that of the femur. Limbs used in locomotion play a critical role in supporting an animal's body mass against gravity. This has been demonstrated by strength of the relationship between femoral and humeral shaft circumference and body mass in extant quadrupeds (femur and humerus) and bipeds (femur only) [17, 67]. Furthermore, we anticipate

that bipeds, which hold the forelimb in aerial suspension, should be under selection to reduce the mass of the forelimb by reducing its cross-sectional diameter. Both considerations should lead to differences in the proportional thickness of forelimb bones of quadrupeds compared to bipeds.

To test this hypothesis, we compiled a database of mammalian, dinosaurian, and other tetrapod limb measurements by expanding existing sources (mammals: [17] [200 mammal species plus 55 reptiles/amphibians], plus measurements of 44 additional mammal species (total = 244 mammal species); dinosaurs: [2, 39]. We especially reviewed the data for Triassic and Early Jurassic sauropodomorphs, which are the focus of the current work. Our data contain information on at least four independent transitions from quadrupedality to bipedality in mammals (among macropodiform marsupials, *Homo*, dipodine rodents, and the spring hare *Pedetes* [another rodent]). Furthermore, based on examination of natural history videos, we considered *Dendrolagus* (the tree kangaroo) to be a quadruped, capturing a transition from bipedality to quadrupedality among mammals. Our dataset also documents at least three evolutionary transitions from bipedality to quadrupedality in dinosaurs: embodied by the definitively quadrupedal ornithischian clades Thyreophora (Stegosauria + Ankylosauria) and Ceratopsidae (e.g. [23]), and the definitive quadrupedal sauropodomorph clade comprising *Vulcanodon* and all more derived sauropods [7]. Most bipedal taxa in the dataset are relatively small-bodied (smaller than *Homo*). However, larger-bodied definite bipeds are present within all three dinosaur clades, and are shown in Figure S3: Ornithischia (e.g. *Thescelosaurus neglectus*, 340 kg; bipedal according to [71, 76], Sauropodomorpha (e.g. *Plateosaurus*, 920 kg; bipedal according to [77], and especially Theropoda (all theropod dinosaurs are bipeds, and Theropoda includes the largest bipedal animals known ([67]: e.g. *Tyrannosaurus rex*, 7.7 tonnes; body mass estimates from [2]). Extinct taxa with uncertain stance (e.g. all iguanodontian ornithischians, including hadrosauroids; non-ceratopsid ceratopsians;

'transitional' sauropodomorphs (indicated on Figure S3), and a giant ground sloth (*Glossotherium*) were labelled as uncertain and excluded from use as predictor variables in our analyses.

Examination of the data suggests a clear split in the relationship between humeral shaft minimum circumference and femoral shaft minimum circumference, with quadrupedal mammals, ornithischians and sauropodomorphs having proportionally robust humeri compared to bipedal members of the same clades (Figures 3, S3). Furthermore, the actual values of these relationships across independent evolutionary transitions from quadrupedality to bipedality (in mammals: apes, rodents, marsupials) and from bipedality to quadrupedality (in ornithischians, sauropodomorphs and *Dendrolagus*) appear consistent (Figure S3). Qualitatively, this suggests that even phylogenetically distant clades of tetrapods achieve quadrupedality by the same proportional increase in humeral shaft robustness, a hypothesis that we test below using regression and discriminant function analysis.

In contrast to the relationship between humeral and femoral shaft circumferences, the relationship of humeral length to femoral length shows little or no apparent distinction between quadrupeds and bipeds among dinosaurs (Table S1; we do not have access to comparable data for other tetrapods). For example, bipedal ornithischians have a similar relationship between humeral and femoral length to that of quadrupedal ornithischians, and theropod dinosaurs (all bipeds) occupy essentially the full range of proportions seen among other dinosaurs of comparable size, regardless of stance. A related metric, forelimb length:hindlimb length, was proposed as a correlate of stance in ornithopods by Galton [70], but was found to be of equivocal use in distinguishing bipeds from quadrupeds among ornithischians by Maidment and Barrett [23, 71]. This contrasts with the apparent distinction between bipeds and quadrupeds shown in the relationship of humeral shaft circumference to femoral shaft circumference

(Figure S3), and is consistent with qualitative observations such as the occurrence of proportionally short forelimbs in some ornithischian dinosaurs, especially stegosaurs [78].

Quantitative hypothesis tests. We tested the hypothesis that bipeds and quadrupeds have distinct relationships between the minimum circumference of the humeral shaft and that of the femur by comparison of phylogenetic generalized least squares [79] linear regression models using information criteria (Akaike's information criterion for finite sample sizes; AICc [66]. These models capture the relationship between $\log_{10}$-transformed humeral shaft minimum circumference and femoral shaft minimum circumference, optionally including variables describing stance (bipedal|quadrupedal; with taxa having undetermined stances excluded from the analysis) and clade membership (Ornithischa|Sauropodomorpha|Theropoda). For this analysis, sauropods with unequivocal quadrupedal stances and columnar forelimbs were classified as quadrupeds (i.e. *Vulcanodon* and more apical sauropods), whereas *Massospondylus* and all more basally-diverging taxa were classified as bipeds (based on evidence in [77] for *Plateosaurus* and [72, 80] for *Massospondylus*. Other sauropodomorphs were classified as uncertain and therefore not used in this analysis. Among ornithischians, thyreophorans (stegosaurs + ankylosaurs) and ceratopsids are regarded unequivocally as quadrupeds (reviewed by [23] and were classified as such. It is also likely that many non-ceratopsid ceratopsians, and many iguanodontians, including hadrosauroids, were quadrupeds. But this is controversial, and they were omitted from our classification. Other ornithischians were classified as bipeds (Barrett & Maidment 2017). All theropod dinosaurs were classified as bipeds; only *Spinosaurus*, for which we do not have limb measurements, was hypothesized as a quadruped by [81].

Phylogenetic generalized least squares (assuming Brownian motion-like evolution of the relationship between variables) is mathematically analogous to ordinary least squares regression of independent contrasts [65] and was implemented using the R packages ape version 4.1 and

nlme version 3.1-131; [45]. For these analyses, we used the distribution of time-calibrated dinosaur phylogenies of [39, 44]; minimum branch length = 1), and allowed λ, a phylogenetic signal parameter [82] to be estimated during the model-fitting process using maximum likelihood. We show results from analysis of just one such tree. But these are representative of analyses conducted over multiple trees with different configurations of branch lengths.

This analysis shows that a model explaining humeral shaft minimum circumference in terms of femoral shaft minimum circumference and stance (bipedal|quadrupedal) was overwhelmingly supported, with an AICc weight of 0.998 (Table S1) and intermediate phylogenetic signal (λ = 0.52). Within this model, the coefficient of femoral shaft minimum circumference is 0.958, indicating either very weak negative allometry or isometry of the robustness of the femur with increasing humeral robustness in dinosaurs. The stance covariate has a statistically significant and positive coefficient indicating that evolutionary transitions from bipedality to quadrupedality in dinosaurs are accompanied by an increase in the proportional robustness of the humerus (Table S1). Removing the stance covariate from this model results in substantially worse AICc. Furthermore, adding clade assignment (Ornithischia|Sauropodomorpha|Theropoda) makes the model worse, and clade categories have non-significant coefficients (Table S1).

We also conducted the same pGLS analysis to examine whether the relationship between $\log_{10}$-transformed humeral and femoral lengths varied between bipeds and quadrupeds among dinosaurs. They do not: the best regression model includes only femoral length (FL) as an explanation of humeral length (HL), and does not include either stance or clade assignment as a covariate (Table S2). Although a model including stance as a covariate has a non-negligible AICc weight, the coefficient of stance in this model is marginally non-significant (Table S2). This, combined with the observation of substantial overlap in the relationship of HL and FL among bipedal and quadrupedal dinosaurs, indicates that this comparison of the lengths of the

humerus and femur does not discriminate well between dinosaurs with different stances and should not be used as an osteological indicator of stance. Furthermore, phylogenetic signal in the relationship between HL and FL is high ($\lambda \sim 0.86$) compared to that for HC and FC ($\lambda = 0.52$; Table S1) indicating that the relationship varies across the phylogeny of dinosaurs and may provide worse predictions of stance when phylogenetic information is not available, or for clades outside the scope of the present analysis (e.g. mammals).

Inference of stance in *Ledumahadi mafube* and other non-sauropodan sauropodomorphs

To provide a predictive framework for inferring the stance in dinosaurs for which this inference cannot otherwise be made unambiguously, we conducted a linear discriminant analysis of our limb measurement dataset. The resulting function is summarized in Tables S2 and S3. This was conducted using the function lda() from the R package MASS [46].

To test the robustness of our initial assignments of taxa to the stance classes (bipedal | quadrupedal), we used 'leave-out-one' cross-validation. This returned 100% confirmatory classifications of the taxa included in our analysis (i.e. all taxa were assigned posteriorly to their correct classes). We also tested the classification based on dinosaurs by attempting predictions of the (known) stances of those extant tetrapods from our dataset that were within the size range of our dinosaurs (N = 97, predominantly mammals; minimum femoral circumference = 34 mm; minimum humeral circumference = 20 mm). The analysis was restricted in this way to avoid extrapolating outside the range of the original data, which would be expected to introduce errors.

In total, the stances of ten extant tetrapods were misclassified (10.3% misclassification) based on our discriminant function for dinosaurs. Confident misclassifications include three rodents, two bovids, one primate, two marsupials and a crocodilian (Table S3), all of which are

quadrupeds that were misclassified as bipeds based on the relationship between the minimum shaft circumferences of their femora and humeri (Table S3). This analysis informs our understanding of the performance of our method: quadrupeds can (rarely) have biped-like proportions, but no instances are known in which bipeds have quadruped-like proportions. Therefore, our method can be used to reject the possibility of bipedality in extinct taxa when quadruped-like proportions are present, but cannot be used confidently to reject the possibility of quadrupedality when biped-like proportions are present. This is also consistent with the observation that some large iguanodontian dinosaurs, including hadrosauroids, have slender, biped-like forelimbs and humeri (gray discs at large body size in Figure S3: A), but also possess many of the osteological correlates of quadrupedality [71], and show evidence of quadrupedality in fossil trackways [23, 83].

Next, we used the results of the linear discriminant analyses to infer the stances of those sauropodomorphs for which stance was not known, and for which measurements of the humerus and femur were available. Data sources for these specimens are described below, and we believe that this represents the most complete sample of transitional sauropodomorphs that could be obtained after excluding specimens from bonebeds, in which the femora and humeri could have come from individuals of different sizes (e.g. *Lessemsaurus*, [11], or for which only the femur (e.g. *Eucnemesaurus entaxonis* [84]), only the humerus (e.g. *Seitaad*, [85]), or neither (e.g. *Blikanasaurus*; [86]), were known. The results of linear discriminant classification of sauropodomorphs are shown in Tables S2 and S3, and in Figure 2.

DATA AND SOFTWARE AVAILABILITY

All data used in this study, including: sauropodomorph measurements, new mammalian measurements, modified data from Campione and Evans 2012, modified data from Benson et al 2017, timescaled dinosaur trees, nexus files and tnt files, and estimates of sauropodomorph

body masses, are available at the following doi:

https://osf.io/hufya/?view_only=dfff4c3bc72b4b8ba2f9a7a858a94b8c.

Data S1. **Appendicular and vertebral measurements of BP/1/7120 (in mm). Related to Figure 2.**

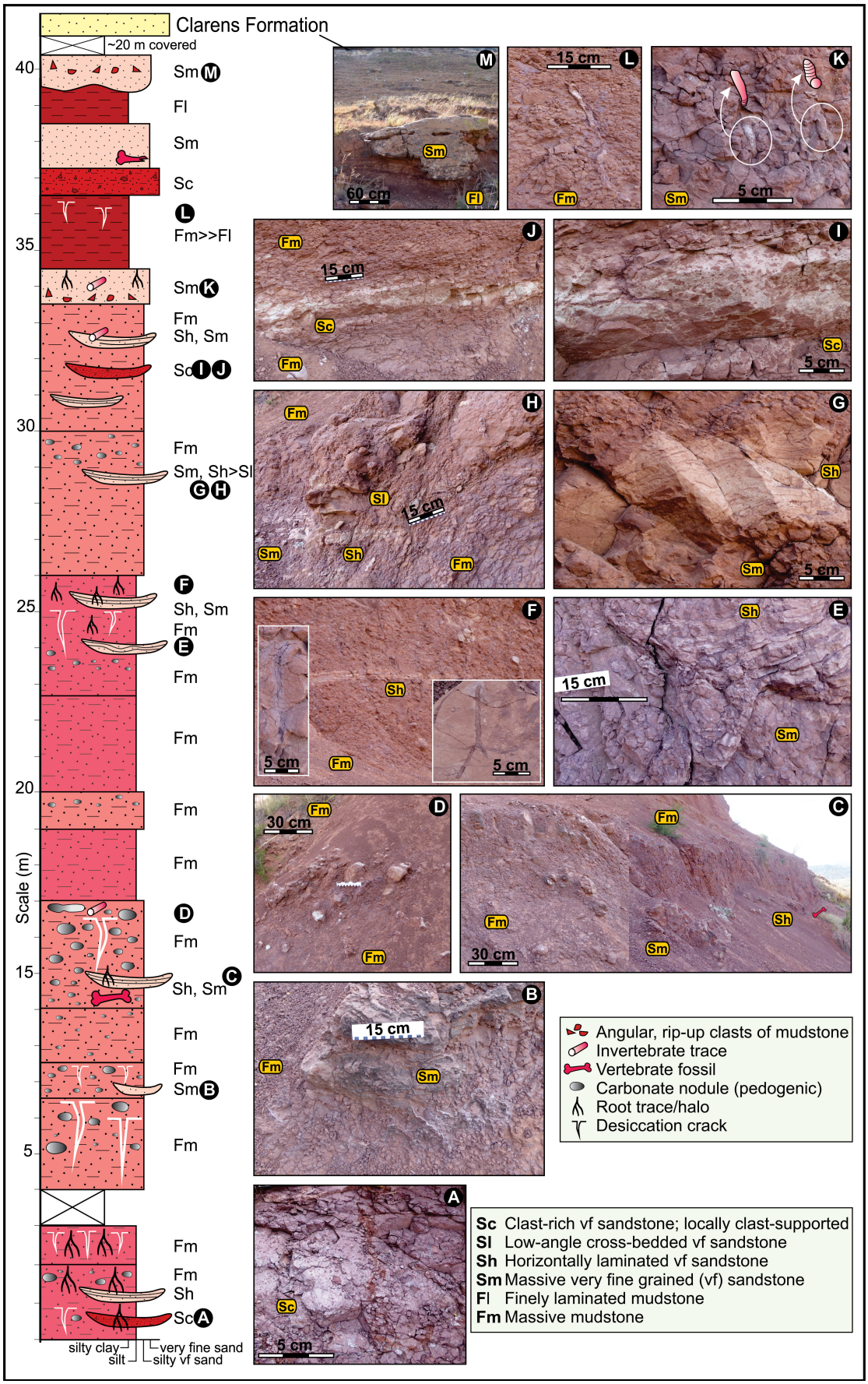
Clarens Formation
~20 m covered
Scale (m)
40
35
30
25
20
15
5
Sm M
Fl
Sm
Sc
L
Fm>>Fl
Sm K
Fm
Sh, Sm
Sc I J
Fm
Sm, Sh>Sl
G H
F
Sh, Sm
Fm
E
Fm
Fm
Fm
D
Fm
Sh, Sm C
Fm
Fm
Sm B
Fm
Fm
Fm
Sh
Sc A
silty clay
silt
very fine sand
silty vf sand
M
Sm
60 cm
Fl
15 cm L
Fm
K
Sm
5 cm
J
Fm
15 cm
Sc
Fm
I
Sc
5 cm
H
Fm
Sl
15 cm
Sm
Sh
Fm
G
Sh
Sm
5 cm
F
Sh
5 cm
Fm
5 cm
E
Sh
15 cm
Sm
D
Fm
30 cm
Fm
C
Fm
Fm
Sh
30 cm
Sm
B
15 cm
Fm
Sm
A
Sc
5 cm
Angular, rip-up clasts of mudstone
Invertebrate trace
Vertebrate fossil
Carbonate nodule (pedogenic)
Root trace/halo
Desiccation crack
Sc Clast-rich vf sandstone; locally clast-supported
Sl Low-angle cross-bedded vf sandstone
Sh Horizontally laminated vf sandstone
Sm Massive very fine grained (vf) sandstone
Fl Finely laminated mudstone
Fm Massive mudstone

Figure S1. Sedimentology of the upper Elliot Formation at Beginsel 346, related to Figure 1 and STAR Methods. Note abundant mudstones with well-developed pedogenic alteration features, in-situ carbonate nodules, root traces, and desiccation cracks. Recurring clast-rich, very fine-grained sandstones, unique UEF facies, are common. The *Ledumahadi* material occurs ~45 m below the base of the Clarens, and ~15m above the base of the UEF. In (**A**): Clast-rich, very fine-grained sandstone (facies Sc) contains poorly sorted, 1-4 cm angular, rip-up mudstone clasts as well as 10-30 cm long, mostly vertical root haloes indicative of pedogenic alternation. A typical sedimentary facies in the UEF associated with sediment gravity flow into smaller, rainstorm-eroded gullies and other irregular depressions of the floodplain. In (**B**): Massive mudstones with small-scale desiccation cracks overlain by a localized lens of massive, very fine-grained sandstone. These fairly common lenticular to irregular interbedded sandstone bodies are 1-2 m wide and <0.5 m thick and probably represent rapid, short-lived deposition in streams/creeks on the floodplain. In (**C, D**): Immediate context of the *Ledumahadi* material reveals a mainly mudstone host rock with a well-developed pedogenic assemblage of in situ pedogenic nodules, which show vertical increase in size and abundance (**D**); interbedded lenticular sandstone bodies, which are either horizontally laminated or massive and localized; deeply penetrating desiccation cracks and root traces (see **F**) as well as smooth- sided, cylindrical invertebrate traces (see **K**). In (**E**): Some of the interbedded lenticular sandstone bodies show soft sediment deformation features, and thus indicate rapid deposition. F: Vertical root traces that taper and branch downwards. Their diameter varies from 0.1 to 10 mm, and the main structures may terminate in multiple branching filamentous root hairs (left inset in **F**). Commonly, root traces have purple-maroon reduction/alteration haloes (right inset in **F**), and cross-cut the entire thickness of the interbedded lenticular sandstone bodies. The root traces are more common and penetrate deeper (up to 80 cm) across all rock types in the upper part of the section, which might indicate better-drained, nonetheless semi-arid soils. In (**G–I**): interbedded lenticular sandstone bodies (**H, J**) show evidence for relatively higher energy depositional processes. These range from horizontal lamination, low-angle cross-bedding to massive beds (**G**, **H**) as well as an abundance of rip-up mudstone clasts, which may be clast-supported locally (**J, I**). Note the cluster of in-situ pedogenic nodules in facies Fm (massive mudstone) indicative of pedogenic overprinting. In (**K**): Typical invertebrate traces in this section are slightly curving to straight, mainly vertical, non-branching, unlined, unornamented, cylindrical tubes of 0.5 cm in diameter and <3 cm in length. They are filled with massive, silty, very fine-grained sandstone and typically occur in isolation as separate tubes (i.e., not as clusters), especially in the upper part of the interbedded lenticular sandstone bodies. Tentatively, they may be interpreted as traces of insects that formed part of the soil biota. In (**L**): Deep penetrating desiccation cracks are the only sedimentary feature in this massive to laminated mudstone, and this it might indicate deposition in a shallow, drying pond. In (**M**): The strong incision of massive sandstone beds (with rip-up clasts) into the underlying laminated mudstones (?pond sediments) is evidence for higher energy, stream process in this part of the log. Also note the broken bone fragment and the overall higher abundance of sandstones with rip-up clasts collectively suggesting a more energetic sedimentary setting.

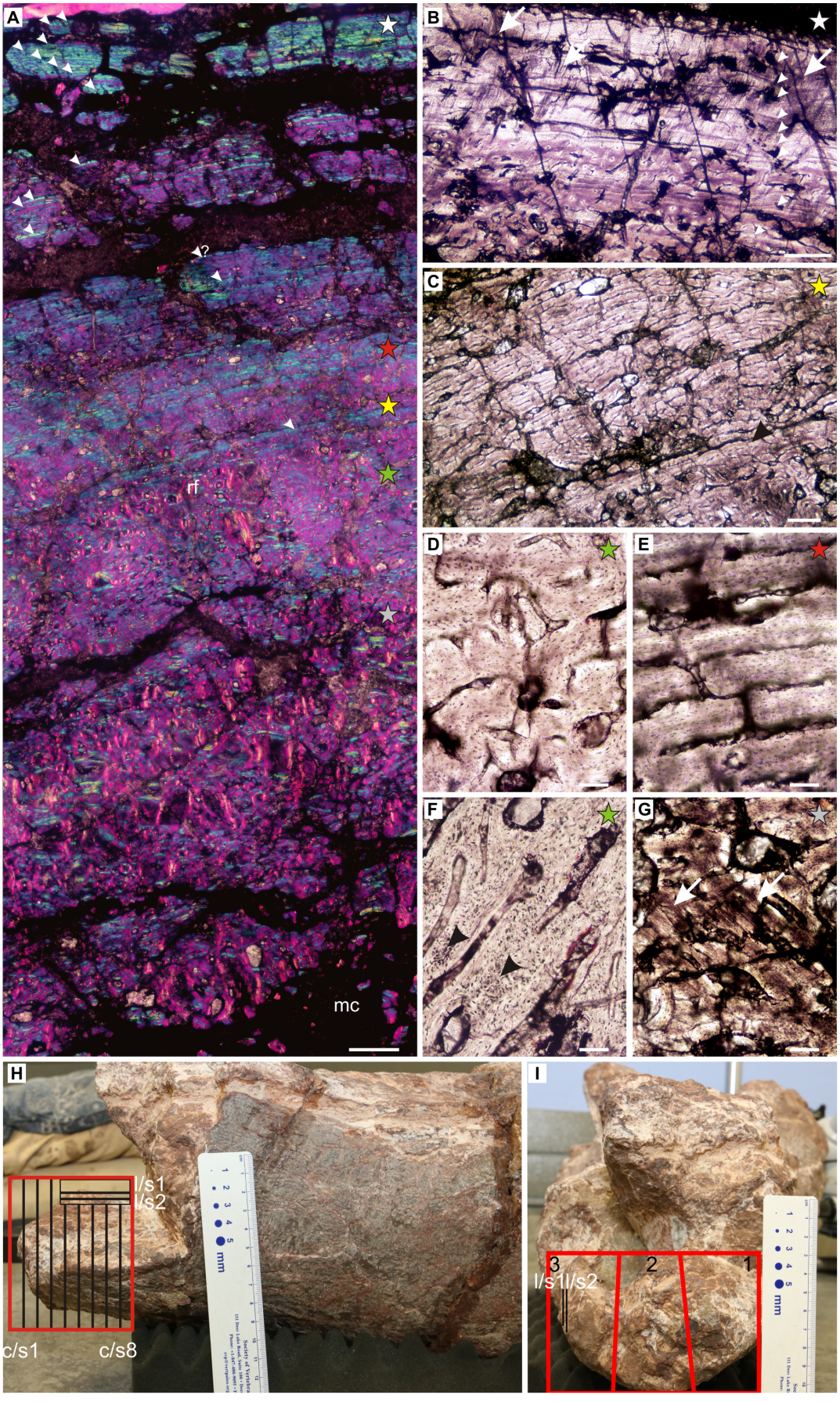
A
B
C
D
E
F
G
H
I
?
rf
mc
l/s1
l/s2
c/s1
c/s8
mm
3
2
1
l/s1
l/s2

Figure S2. Osteohistological thin-sections of *Ledumahadi*, related to Figure 1, STAR Methods. In (**A**): transition from fibrolamellar bone (predominantly pink) to peripheral lamellar-zonal bone (predominantly blue). Growth marks (arrowheads) appear in the outer half of the cortex (arrowheads with question marks are uncertain annuli). The resorption front (rf) is limited to the inner half of the cortex. In (**B**): peripheral slowly forming lamellar-zonal bone with multiple LAGs (arrowheads). Arrows indicate Sharpey's fibers. In (**C**): laminar fibrolamellar bone tissue. Arrowhead marks the first visible annulus in the cortex. In (**D**): haphazardly arranged globular osteocyte lacunae between longitudinally-oriented primary osteons transitioning to (**E**): predominantly flattened osteocyte lacunae with little space between the osteonal lamellae. In (**F**): longitudinal section showing the presence of large, clustered, globular osteocyte lacunae in a woven-fibered matrix (arrowheads). In (**G**): prominent Sharpey's fibers (arrows), which extend deep into the cortex. Matching stars indicate the area of the cortex from where each image was taken. In (**H, I**): approximate postions of osteohistological cross-sections and longitudinal sections on the femur of *Ledumahadi* in (**H**) lateral view, (**I**), proximal view; red lines denote boundaries of overall section, arabic numerals in (**I**) denote subsections. Abbreviations: c/s, cross-section; l/s, longitudinal section; mc, medullary cavity; rf, resorption front. Scale bars equal 2 mm (**a**); 500 μm (**b, c**); 100 μm (**d–g**).

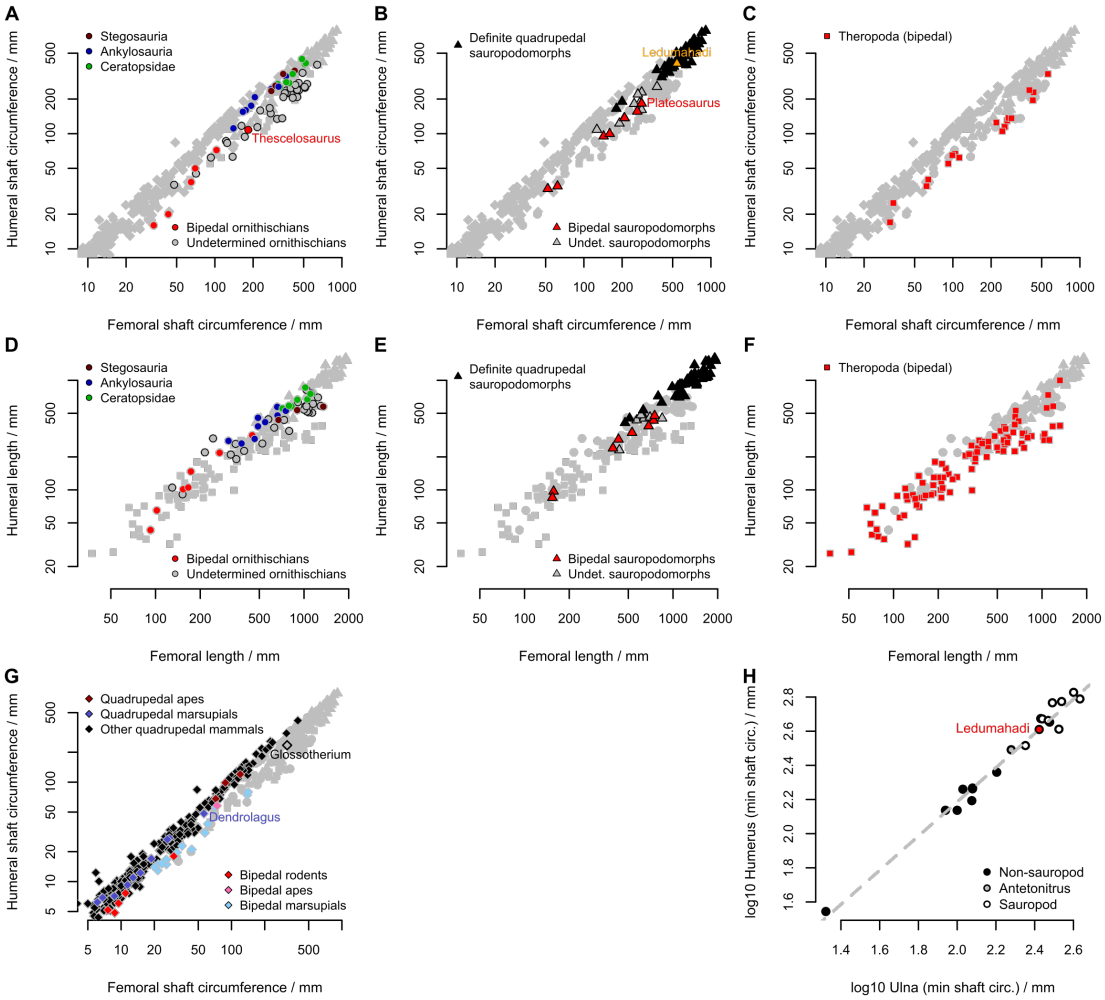

Figure S3. Summary of regression data, related to Figure 3, STAR Methods. In (**A–C**, **G**): relationship between (log10-transformed) humeral minimum shaft circumference and femoral minimum shaft circumference for (**A**) ornithischian dinosaurs [N = 57], (**B**) sauropodomorph dinosaurs [N = 59], (**C**) theropod dinosaurs [N = 19], and (**G**) mammals [N = 233] plus extant reptiles/amphibians [N = 55]. In (**D-F**): relationship between (log10-transformed) humeral length and femoral length for (**D**) ornithischian dinosaurs [N = 58], (**E**) sauropodomorph dinosaurs [N = 66], and (**F**) theropod dinosaurs [N = 100]. In (**H**): regression of humeral minimum shaft circumference on ulnar minimum shaft circumference in sauropodomorphs used to estimate the minimum shaft circumference of the missing humerus of *Ledumahadi mafube* (red datapoint). Gray dashed line is the ordinary least squares (OLS) regression line (y = 1.000*x + 0.0875; pslope <0.0001 ; N = 17). In panels (**A-G**), points are colored according to locomotory status. See top-left legends for quadrupedal taxa and bottom-right legends for bipeds. In each of thee panels, the full set of all points for all clades is shown as gray, unbounded shapes in the background of each plot.

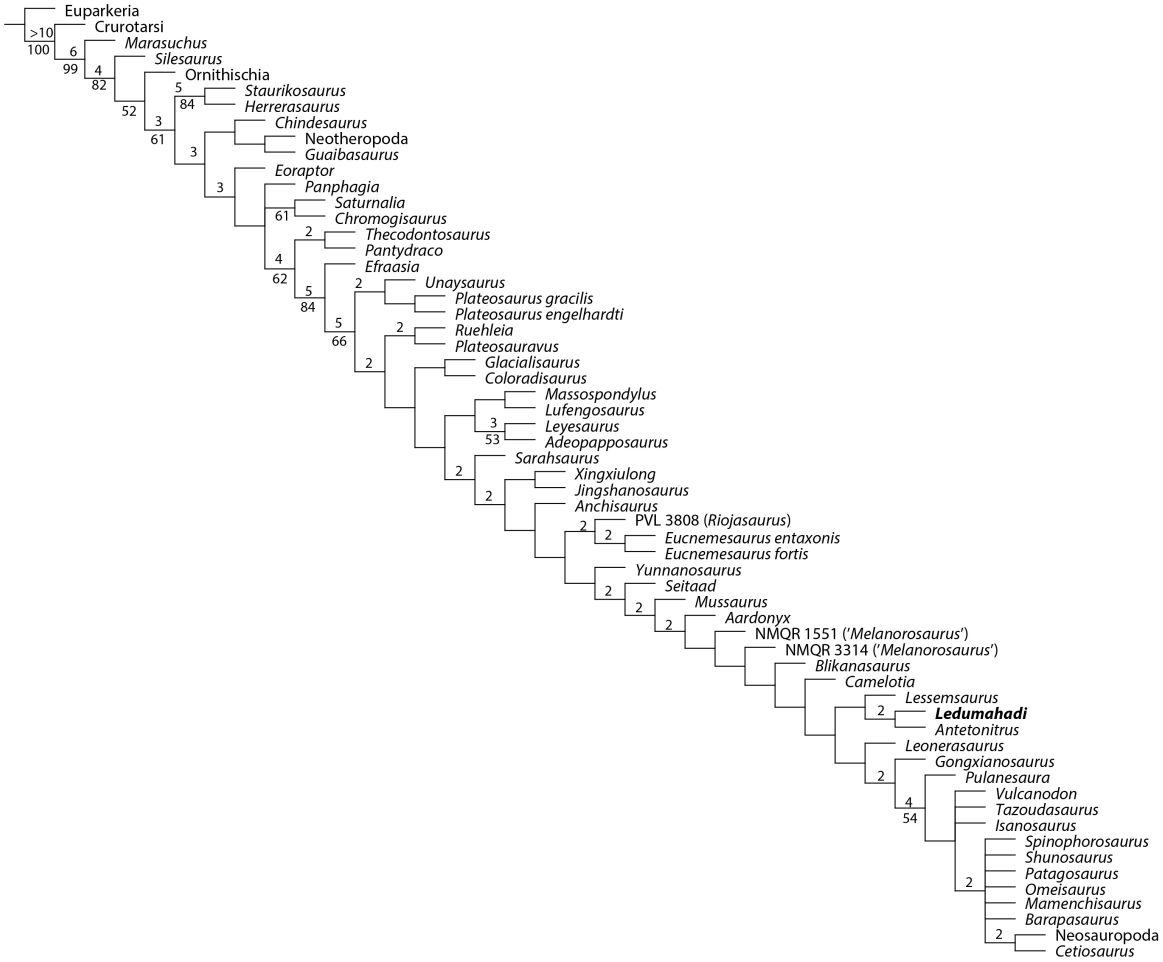

Figure S4. Strict consensus of 6 MPTs derived from phylogenetic analysis protocol, related to Figure 2, STAR Methods. Length of MPTs equals 1286, CI: 0.338; RI: 0.688. Numbers above branch represent Bremer supports (>1). Numbers below branch represent bootstrap score (>50%).

Model	AICc	AICc weight	λ	R^2	Variable	Slope	p-value
Humeral circumference (HC) models:							
HC ~ FC + stance	**225.2**	**0.998****	0.52	0.94	(Intercept)	-0.139	0.005
					log10(FC)	0.958	<0.001
					Quadrupedal	0.171	<0.001
HC ~ FC + stance + clade	-212.8	0.002	0.66	0.94	(Intercept)	0.183	0.005
					log10(FC)	0.957	<0.001
					Quadrupedal	0.182	<0.001
					Sauropodomorpha	0.051	0.256
					Theropoda	0.038	0.524
HC ~ FC	-206.2	<0.001	0.85	0.93	(Intercept)	-0.25	<0.001
					log10(FC)	1.02	<0.001
HC ~ FC + clade	-194.9	<0.001	0.87	0.92	(Intercept)	-0.281	0.001
					log10(FC)	1.022	<0.001
					Sauropodomorpha	0.03	0.652
					Theropoda	-0.005	0.956
Humeral length (HL) models:							
HL ~ FL	**-290.4**	**0.821****	0.88	0.89	(Intercept)	-0.086	0.204
					log10(FL)	0.943	<0.001
HL ~ FL + stance	**-287.3**	**0.174***	0.86	0.89	(Intercept)	-0.053	0.443
					log10(FL)	0.926	<0.001
					Quadrupedal	0.086	0.067
HL ~ FL + clade	-280	<0.001	0.88	0.89	(Intercept)	-0.073	0.488
					log10(FL)	0.947	<0.001
					Sauropodomorpha	-0.023	0.796
					Theropoda	-0.07	0.495
HL ~ FL + stance + clade	-276.5	<0.001	0.86	0.89	(Intercept)	-0.054	0.6
					log10(FL)	0.93	<0.001
					Quadrupedal	0.083	0.086
					Sauropodomorpha	-0.008	0.928
					Theropoda	-0.049	0.629

Table S1. **Summary of phylogenetic generalized least squares (pGLS) results for models of the relationships of humeral minimum shaft circumference (HC) and humeral length (HL), related to Figures 2, 3, S3, STAR methods.** Explanatory variables include femoral minimum shaft circumference (FC), stance (bipedal|quadrupedal) and clade identity (Sauropodomorpha|Theropoda|Ornithischia). Measurements are $\log_{10}$-transformed. N = 82 for all analyses. R^2 is the generalized R^2 of [S1] by comparison to an intercept-only null model. The best model is indicated by bold type and double-asterisks by its AICc weight. Single-asterisks indicate non-negligible AICc weights.

	Bipedal	Quadrupedal
Prior probabilities	0.346	0.654
Group means		
log10(FC)	2.185	2.659
log10(HC	1.947	2.575
Coefficients of linear discriminants		
log10(FC): 16.4401		
log10(HC: 19.6897		

Table S2. Summary of linear discriminant function based on analysis of N = 81 dinosaurs in this study. Related to Figure 3, STAR Methods, Data S1.

Taxon	Bipedal	Quadrupedal	Inference	Actual
Sauropodomorphs				
Yunnanosaurus	0.983	0.017	biped	-
Anchisaurus	0.311	0.689	likely quadruped	-
Jingshanosaurus	0.085	0.915	quadruped	-
Xingxiulong	<0.001	>0.999	quadruped	-
Riojasaurus (PVL 3808)	0.001	0.999	quadruped	-
Mussaurus	0.999	0.001	biped	-
NMQR 3314	0.075	0.925	quadruped	-
Antetonitrus	0.001	0.999	quadruped	-
Ledumahadi	<0.001	>0.999	quadruped	-
Extant tetrapods				
Rodents				
Castor canadensis	1	<0.001	biped	quadruped
Dolichotis patagonum	0.998	0.002	biped	quadruped
Erethizon dorsatum	0.999	0.001	biped	quadruped
Bovids				
Sylvicapra grimmia	1	<0.001	biped	quadruped
Hydropotes inermis	0.998	0.002	biped	quadruped
Xenarthra				
Choloepus hoffmanni	0.503	0.497	ambiguous	arboreal quadruped
Primates				
Ateles paniscus	0.997	0.003	biped	arboreal quadruped
Marsupials				
Dendrolagus lumholtzi	1	<0.001	biped	arboreal quadruped
Dendrolagus inustus	0.694	0.306	likely biped	arboreal quadruped
Crocodylia				
Caiman crocodilius	0.892	0.108	likely biped	quadruped

Table S3. Linear discriminant classifications of locomotory styles for transitional sauropodomorphs and for extant tetrapods whose stance was misclassified based on the linear discriminant function for dinosaurs. Related to Figure 3, STAR Methods. Posterior probabilities and resulting inferences are given. Only transitional sauropodomorphs of uncertain stance are recorded here. Other taxa were fixed as bipedal (e.g. *Sarahsaurus*, *Massospondylus*, *Lufengosaurus*, *Ruehleia*, *Plateosaurus*, *Saturnalia*) or quadrupedal (Sauropoda), and 100% of these assignments were validated posteriorly by leave-one-out resampling. Among extant tetrapods, of a total N = 97 species within the body size range of dinosaurs, ten were misclassified, and all confident misclassifications (nine in total) were of quadrupeds misclassified as bipeds.

Supplemental References

S1. Nagelkerke, N.J. (1991). A note on a general definition of the coefficient of determination. Biometrika *78*, 691-692.